Palaeoenvironmental changes in the southwestern Mediterranean (ODP site 976, Alboran sea) during the MIS 12/11 transition and the MIS 11 interglacial and implications for hominin populations

Dael Sassoon, Vincent Lebreton, Nathalie Combourieu-Nebout, Odile Peyron, Marie-Hélène Moncel

Title: Palaeoenvironmental Changes in the Southwestern Mediterranean (ODP Site 976, Alboran Sea) During the MIS 12/11 Transition and the MIS 11 Interglacial and Implications for Hominin Populations

Authors: Dael SASSOON[1]*, Vincent LEBRETON[1], Nathalie COMBOURIEU-NEBOUT[1], Odile PEYRON[2], Marie-Hélène MONCEL[1]

Affiliations:
1: Muséum national d'Histoire naturelle, UMR 7194 Histoire Naturelle de l'Homme Préhistorique, Paris
2: Institut des Sciences de l'Évolution de Montpellier, UMR 5554, Université de Montpellier

** corresponding author*

Palaeoenvironmental Changes in the Southwestern Mediterranean (ODP Site 976, Alboran Sea) During the MIS 12/11 Transition and the MIS 11 Interglacial and Implications for Hominin Populations

Dael SASSOON[1*], Vincent LEBRETON[1], Nathalie COMBOURIEU-NEBOUT[1], Odile PEYRON[2], Marie-Hélène MONCEL[1]

[1]Muséum national d'Histoire naturelle, UMR 7194 Histoire Naturelle de l'Homme Préhistorique, Paris

[2]Institut des Sciences de l'Évolution de Montpellier, UMR 5554, Université de Montpellier

Abstract

The transition from the Marine Isotope Stage (MIS) 12 glacial (ca. 478–424 ka BP) to the MIS 11 interglacial (ca. 424–365 ka BP) is one of the most remarkable climatic shifts of the Middle Pleistocene and is regarded as a phase of major behavioural innovation for hominins. However, many of the available pollen records for this period are of low resolution or fragmented, limiting our understanding of millennial-scale climatic variability. We present a high-temporal resolution pollen record that encompasses the period between MIS 12 and MIS 10 (434–356 ka BP), recovered from the Ocean Drilling Program (ODP) Site 976 in the Alboran Sea. This study aims to provide new insights into the response of vegetation during the transition and to highlight patterns of climatic variability during MIS 11.

The ODP Site 976 pollen record shows the shift from glacial to interglacial at 426 ka BP, highlighted by the transition from *Pinus*, herbaceous and steppic taxa to temperate and Mediterranean taxa. A climatic optimum for temperate and Mediterranean taxa is identified around 426–400 ka BP, equivalent to substage MIS 11c and synchronous with the maxima in SSTs, greenhouse gas concentrations and insolation. A phase with increased *Pinus* and *Cedrus* indicates the return to colder and more arid conditions during substage MIS 11b (400–390 ka BP). Substage MIS 11a (390–367 ka BP) is marked by a period of short-term warming followed by gradual cooling, until the return of glacial conditions during MIS 10. Forest contractions have been linked with high- and moderate-intensity climate events also observed in other pollen records and proxies from the Mediterranean and North Atlantic.

Our results confirm the intense shift during the MIS 12/11 transition and show that this region is sensitive to millennial-scale climatic variation during MIS 11. The forest contractions observed in our record during events of millennial-scale variability appear to be less intense than in the central and eastern Mediterranean. This suggests that the southwestern Mediterranean may have been less variable during periods of climatic deterioration, thereby representing a possible ecological niche for vegetation. This may have provided a source of subsistence for hominins during harsher conditions, thus contributing to their demographic expansion and technological innovations.

Keywords: Southwestern Mediterranean; Middle Pleistocene; Marine record; Pollen; Vegetation dynamics; Long-term vegetation change; Climate change; Millennial-scale climate variability

1. Introduction

The transition from the extensive glaciation of MIS (Marine Isotope Stage) 12 to the remarkably long and warm MIS 11 interglacial is regarded as one of the most extreme climatic shifts over the last 900 ka (Chaisson *et al.*, 2002; Tzedakis *et al.*, 2009; Sánchez Goñi *et al.*, 2016; Marino *et al.*, 2018). This shift, occurring during Termination V (TV), stands out in the

Middle Pleistocene due to the exceptional increase in sea levels and greenhouse gas concentrations from MIS 12 to MIS 11 despite minimal astronomical forcing—what Berger and Wefer (2003) defined as the "Stage-11 Paradox". In marine and terrestrial records, the MIS 12 glacial (ca. 478–424 ka BP) is often deemed as one of the most severe glacial periods of the Pleistocene, during which the global ice volume exceeded that of the Last Glacial Maximum (LGM) and the European ice sheet reached its maximum of the last 1.2 Ma (Olson and Hearty, 2009; Toucanne *et al.*, 2009; Koutsodendris *et al.*, 2019). Pollen records from Tenaghi Philippon (e.g. Tzedakis *et al.*, 2006; Pross *et al.*, 2015) and Lake Ohrid (Sadori *et al.*, 2016; Kousis *et al.*, 2018) show that this period was characterised by severe reductions in tree populations associated with a prevalence of cold conditions. In contrast, especially warm and humid conditions prevailed during MIS 11 (ca. 424–365 ka BP) even in the higher latitudes of the Northern Hemisphere (Kousis *et al.*, 2018) over a period longer than any other interglacial of the Mid- to Late Pleistocene (Marino *et al.*, 2018). The climatic optimum during substage MIS 11c has been widely recognised as a long, warm and relatively stable period of the interglacial in both marine and terrestrial records across the Mediterranean, showing that these conditions prevailed across the wider region (e.g. Oliveira et al; 2016; Kousis *et al.*, 2018; Azibeiro *et al.*, 2021). Such a long-lasting interglacial period after the harsh glacial conditions of MIS 12 favoured the development of temperate vegetation across Europe and in turn led to the demographic expansion of hominin populations (Berger and Loutre, 2003; Raymo *et al.*, 2012; Oliveira *et al.*, 2016; Moncel *et al.*, 2018).

Indeed, from a hominin evolution point of view, the MIS 12/11 transition represents a significant threshold period. Genetic data and anthropological analyses have recently shown that European Neanderthal features emerged in the population between 600 and 400 ka (Hublin, 2009) and that climatic amelioration after the MIS 12 glaciation led to a phase of major innovation for hominins. Archaeological records for this period show evidence of increased occupations, new subsistence behaviours and technical innovations (e.g. core technologies, increase in light-duty tools), and an early regionalization of traditions (Moncel *et al.*, 2016; Blain *et al.*, 2021). Investigating vegetation changes during this period is key to improving our understanding of the impacts of climate on biomass availability for large herbivores, the mobility of human groups and demographic changes.

Furthermore, in recent years MIS 11 has received a noticeable amount of attention as it is regarded as one of the best analogues to the Holocene (MIS 1) (Loutre and Berger, 2003; Candy et al., 2014). Both interglacials, MIS 11 and MIS 1, are characterised by high sea levels, intense warmth, low astronomical forcing—in particular low precession—and elevated atmospheric CO_2 concentrations (McManus *et al.*, 2003; Desprat *et al.*, 2005; Hes *et al.*, 2022). This makes MIS 11 an important period for investigating climatic variability and its impacts on vegetation and hominin populations during conditions similar to those of the current interglacial.

Although the MIS 12/11 transition has been previously studied across the Mediterranean (Fig. 1, Tab. 1) through the use of terrestrial (pollen) and marine climatic indicators (planktic foraminifera and oxygen isotopes), many of the available records are of relatively low-temporal resolution and/or fragmented (e.g. Desprat *et al*., 2005; Tzedakis *et al*., 2009). Thus, our understanding of short-term vegetation change and millennial-scale climatic variability is still limited. Important advances have been recently made with records from the Iberian margin (Desprat *et al.*, 2005, 2007; Oliveira *et al.*, 2016, Hes *et al.,* 2022) and new studies have attempted to increase the resolution of existing records, such as Lake Ohrid (Kousis *et al.*, 2018) and Tenaghi Philippon (Ardenghi *et al*., 2019). These studies have shown the

importance of long records with a high-temporal resolution to better understand the amplitude of centennial-scale changes in temperature, precipitation, and the length of cold episodes. However, more research is required to understand the responses of vegetation to climate and the changes in temperature and precipitation during this transition across the Mediterranean region, especially in the southwestern area where only few and fragmentary terrestrial records are available (e.g. Atapuerca; Rodríguez *et al.,* 2011).

In this study, we present a high-temporal resolution pollen record recovered from the ODP Site 976 in the Alboran Sea that encompasses a long timeframe from MIS 12 to MIS 10 (434–356 ka BP). The continuous, high-resolution pollen data generated in this study allowed the study of millennial-scale vegetation changes and comparisons with other high-resolution pollen and climatic records in the Mediterranean. This study aims to: (1) provide a new high-resolution pollen record encompassing the MIS 12/11 transition; (2) reconstruct regional landscape-scale changes in vegetation; (3) highlight patterns of climate variability in the Mediterranean region; and (4) discuss hominin subsistence in this context.

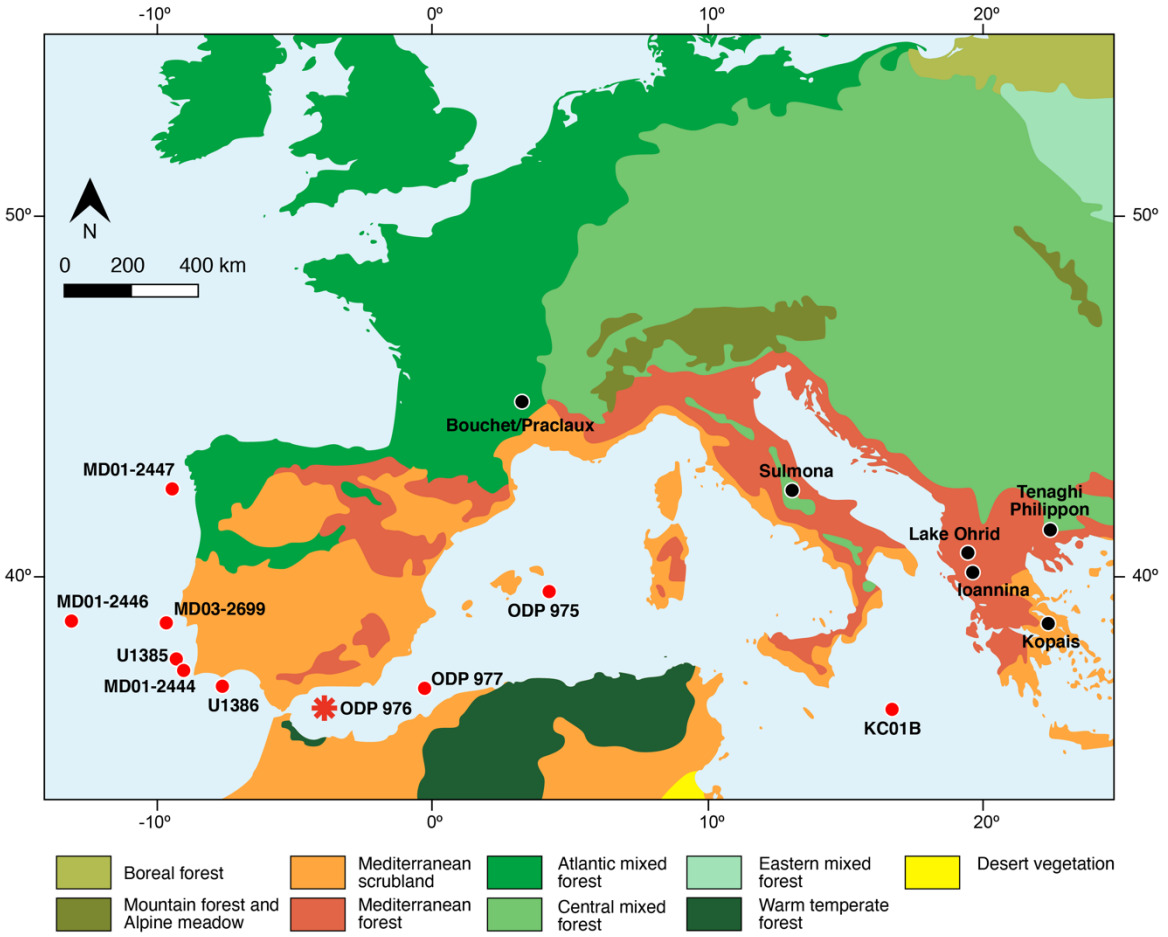

Figure 1 – Map showing the modern vegetation distribution (modified from Sánchez Goñi, 2022). The location of ODP Site 976 is indicated with a red star along with other marine (red dots) and terrestrial (black dots) proxy records covering MIS 12 and 11 discussed in the text. For more information about the sites and proxies used see Table 1.

Table 1 – Terrestrial and marine records from the Mediterranean covering MIS 12 and 11.

Site name	Site type	Lat (°N)	Long (°W)	Elevation (m)	Period (ka BP)	MIS stages	Record type	References

Ioannina	Terrestrial	39.4	20.51	470 asl	500-0	13–1	Pollen	Tzedakis, 1993, 1994; Tzedakis *et al.*, 1997, 2001
IODP U1385	Marine	37.57	-10,12	2578 bsl	440–365	12a–10c	Pollen, alkenones	Oliveira *et al.*, 2016
IODP U1386	Marine	36.83	-7,76	561 bsl	433–404	12a–11d	Pollen	Hes *et al.*, 2022
KC01B	Marine	36.15	17.44	3643 bls	1200–0	36–1	Foraminifera, $\delta^{18}O$	Lourens, 2004
					464–419	12c–11c	Foraminifera, $\delta^{18}O$	Azibeiro *et al.*, 2021
Kopais	Terrestrial	38.37	23.13	95 asl	500–0	13–1	Pollen	Okuda *et al.*, 2001
Lac du Bouchet	Terrestrial	44.55	3.47	1200 asl	450–0	12–0	Pollen	Reille and De Beaulieu, 1995
Lac du Praclaux	Terrestrial	44.49	3.5	1100 asl	450–1	12–1	Pollen	Reille and de Beaulieu, 1990 ; Reille and de Beaulieu, 1995 ; Reille *et al.*, 1998
Lake Ohrid	Terrestrial	41.02	20.42	1514 asl	500–0	13–1	Pollen, foraminifera, $\delta^{18}O$	Sadori *et al.*, 2016; Wagner *et al.*, 2019
					465–430	12a–10c	Pollen, tephra	Kousis *et al.*, 2018
MD01-2444	Marine	37.33	10.08	2637 bsl	430–0	12–0	Foraminifera, $\delta^{18}O$, alkenone	Martrat *et al.*, 2007
MD01-2446	Marine	39.03	12.37	3570 bsl	545–300	14–9	Foraminifera, $\delta^{18}O$	Voelker *et al.*, 2010
					550–290	14–8	Foraminifera, calcareous nanofossil, $\delta^{18}O$	Marino *et al.*, 2014
MD01-2447	Marine	42.15	-9.67	2080 bsl	426–394	12–11	Pollen, foraminifera, $\delta^{18}O$	Desprat *et al.*, 2005, 2007
MD03-2699	Marine	39.02	10.39	1865 bsl	580–300	15–9	Alkenones	Rodrigues *et al.*, 2011
ODP975	Marine	38.53	4.3	2415 bsl	1200–0	36–0	Foraminifera, $\delta^{18}O$	Pierre *et al.*, 1999; Lourens, 2004
					650–250	16–8	Foraminifera, $\delta^{18}O$	Girone *et al.*, 2013
ODP976	Marine	36.12	4.18	1108 bsl	434–357	12a–10c	Pollen	This study
ODP977	Marine	36.01	1.57	1984 bsl	540–300	13c–9a	Foraminifera, calcareous nanofossil, $\delta^{18}O$	Marino *et al.*, 2018; Azibeiro *et al.*, 2021
Sulmona basin	Terrestrial	-	-	360–2000 asl	500–410	13–11	Speleothems, lithology, XRF, CaCO3 content, carbonate $\delta^{18}O$ and $\delta^{13}C$	Regattieri *et al.*, 2016
Tenaghi Philippon	Terrestrial	41.10	24.2	40 asl	440–330	12–10	Pollen, alkenone, brGDGTs, leaf wax, levoglucosan	Ardenghi *et al.*, 2019
					1400–0	42–1	Pollen	Tzedakis *et al.*, 2006
					460–335	12–10	Cryptotephra	Vakhrameeva *et al.*, 2018

2. Regional setting

This study used sections of the long marine sequence recovered during Leg 161 of the Ocean Drilling Program (ODP) (Shipboard Scientific Party, 1996) from ODP Site 976 in the Western Alboran Sea (Fig. 2; 36°12.3'N 4°18.8'W), located about 110 km from the Strait of Gibraltar at 1108 m water depth (Combourieu-Nebout *et al.*, 1999, 2009; Gonzalez-Donoso *et al.*, 2000).

The Alboran Sea, a narrow extensional basin measuring 150 km wide and 350 km in length (Alonso *et al.*, 1999) is a transitional area between the Mediterranean Sea and the Atlantic Ocean (Bulian *et al.*, 2022), and represents the westernmost side of the Mediterranean, bordered by Spain to the north and Morocco to the south.

Circulation in the Alboran Sea is strong, mainly due to the water exchange at the Strait of Gibraltar between the inflow of low-salinity waters from the Atlantic and the outflow of high-salinity Mediterranean waters, which results in two anti-cyclonic gyres known as the Western and Eastern Alboran Gyres (WAG and EAG, respectively) (Bulian *et al.*, 2022). ODP976 is located near the centre of the WAG (Fig. 2).

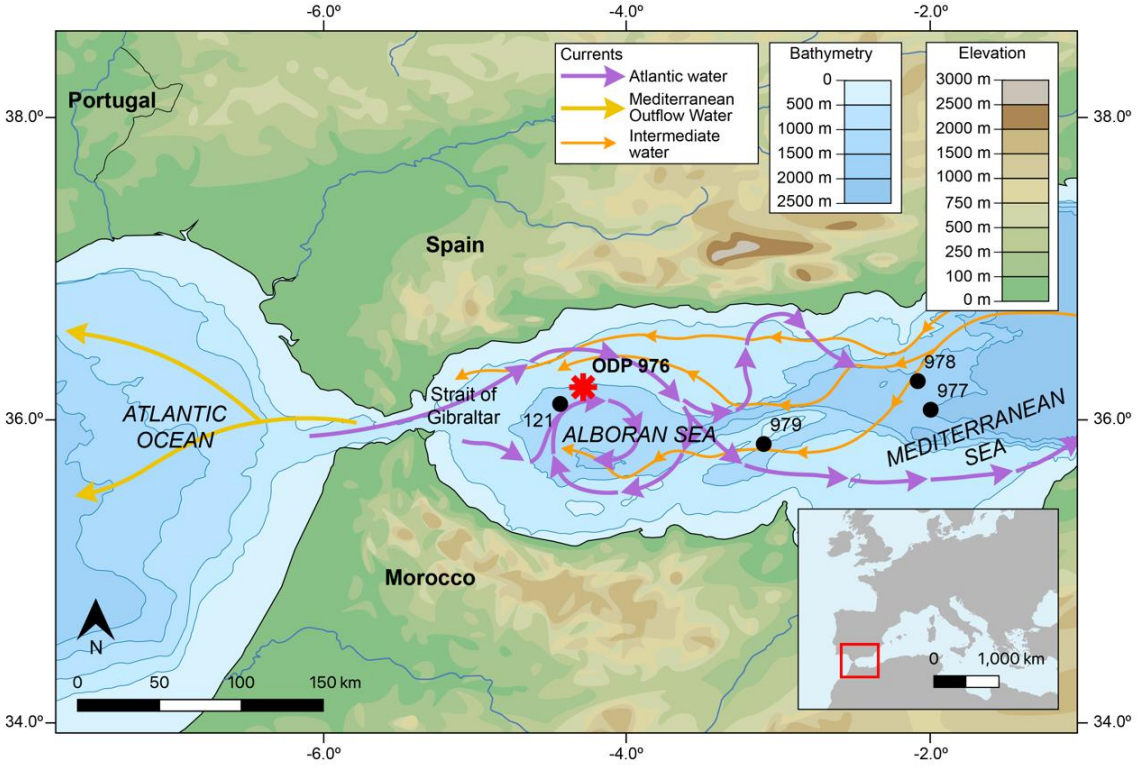

Figure 2 – Map showing the location of ODP Site 976 and the present-day surface and water circulation in the Alboran Sea (modified from Combourieu-Nebout *et al.*, 1999). Other ODP sites are marked with black dots.

The climate in this region is Mediterranean and strongly influenced by the Southern Azores cyclone in summer which results in long, dry summers and mild, rainy winters (Combourieu-Nebout *et al.*, 1999, 2009). Mean temperatures of the coldest months range between 10°C near the coast and -7°C at altitudes above 2000 m, while mean temperatures of the warmest months usually exceed 25°C (Garcia-Gorriz and Garcia-Sanchez, 2007; Parada and Canton, 1998); annual precipitation ranges between 400 and 1400 mm (Combourieu-Nebout *et al.*, 2009).

The landscape is enclosed by the mountains of the Moroccan Rif and Betic Cordillera, leading to an altitudinal range of vegetation (Quézel and Medail, 2003). Steppe vegetation with *Lygeum*, *Artemisia* and a Mediterranean group of taxa including *Olea*, *Phillyrea, Pistacia*, and *Quercus ilex* dominates the coast. This assemblage is replaced by a humid-temperate oak forest with *Quercus deciduous* and Ericaceae at mid-altitudes, and finally by cold-temperate coniferous forests with *Pinus* and *Abies* at higher elevations. Currently, *Cedrus* is typically found in the higher elevations of Morocco (Ozenda, 1975; Rivas Martínez, 1982; Barbero *et al.*, 1981; Benabid, 1982).

The location of ODP976 was chosen because previous studies have shown that the Western Alboran Sea is particularly sensitive to centennial and millennial climate change due to its unique exposure to polar tropical and Atlantic influences (Alonso *et al.*, 1999; Combourieu-Nebout *et al.*, 1999, 2002, 2009; Bulian *et al.*, 2022). It has also been recently the focus of studies on planktonic foraminifera to investigate MIS 12 and 11 by Marino *et al.* (2018) and Azibeiro *et al.* (2021), showing the ability of this location to record climatic variability during this particular period.

3. Material and Methods

3.1 Chronology

3.1.1 Age model

The chronology for this study has been adopted from von Grafenstein *et al.* (1999), who correlated the biostratigraphic marker events in the study by de Kaenel *et al.* (1999) on ODP976 (i.e. changes in the planktonic foraminifera *Globigerina bulloides*) with the benthic oxygen isotope record of Site 659. The ages presented here are in calendar ka (cal ka), consistent with the model developed by von Grafenstein (Fig. 3) and other studies that have adopted this chronology for the ODP976 core (e.g. Combourieu-Nebout *et al.*, 2009). Age interpolation of the record has a maximum age of 433.868 ka BP at 118.8 m and a minimum age of 356.456 ka BP at 98.85 m. Interpolation was achieved with the *interpol* function of *tidypalaeo* on R.

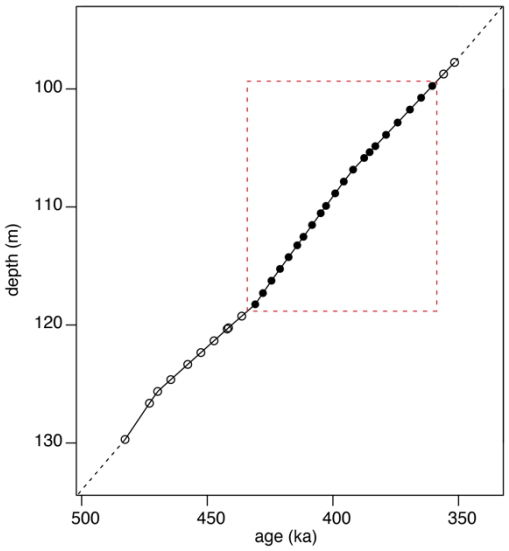

Figure 3 – Age model by von Grafenstein *et al.* (1999). Black dots within the red dotted square highlight the chronological interval adopted for this study.

3.1.2 MIS subdivision

MIS 11 is traditionally divided into three substages: a, b and c (Hrynowiecka *et al.*, 2019). This subdivision has been adopted by most palynological studies in the Mediterranean (e.g. Oliveira *et al.*, 2016; Kousis *et al.*, 2018; Ardenghi *et al.*, 2019). Recent palaeoclimatic studies on MIS 11 in the Northern Hemisphere have introduced two additional substages at the base of MIS 11 (11d and 11e) based on minor changes in isotopic data (Railsback *et al.*, 2015; Hrynowiecka *et al.*, 2019). This distinction seems to be highly dependent on the geographical location of the records, their temporal resolution and the proxies used, and so far only few records have applied a five-substage subdivision—among pollen studies, this partition has been used in the North Atlantic off the coast of Iberia, but not in the Mediterranean. Therefore, we followed the more widely applied nomenclature for MIS 11, defining the base of the interglacial as MIS 11c.

3.2 Pollen analysis

A total of 141 samples were selected from Holes 976 B13, B12 and C12 of the ODP Site 976 marine core (representing the depths 98–119 m, dated between MIS 12 and MIS 10), at an average resolution of 10 cm with occasional higher resolution in specific areas of interest. Samples were dried and 5 g of sediments were treated following standard methods (Faegri

and Iversen, 1989) under 10% HCL, 40% HF and 20% HCL and sieved with a 10 µm sieve (Combourieu-Nebout *et al.*, 2009). Acetolysis was avoided to preserve dinoflagellates. Two *Lycopodium* tablets (batch number: 1031) were added to calculate absolute pollen concentrations (pollen grains per unit of sediment volume).

A minimum of 150 grains of total land pollen (TLP) were counted for each sample, excluding *Pinus* because of their natural overrepresentation in European biomes and marine records (Fletcher and Sánchez Goñi, 2008; Sánchez Goñi *et al.*, 2009; Sadori *et al.*, 2016), as well as aquatics (e.g. *Cyperaceae* and *Typha/Sparganium*) and fungal/algal spores (e.g. Pteridophyta). Ecological groups were based on modern climate-vegetation associations and follow the main groups defined by Suc (1984). Despite having subtropical and temperate affinities respectively, pollen grains of *Carya* and *Euonymus* were found at very low levels (<1.3%) and therefore these taxa were included within the Ubiquist group. A target of 20 morphotypes was chosen to ensure an appropriate representation of vegetation composition.

The percentage pollen diagrams were developed using the *Rioja* package in the software *R* (Juggins, 2020). Taxa were divided into ecological groups representative of specific climatic conditions (Tab. 2).

Table 2 – Taxa included in each ecological group

Ecological group	Taxa
Riparian	*Betula, Alnus, Pterocarya, Fraxinus, Ilex, Salix*
Montane	*Abies, Picea, Cedrus, Tsuga*
Temperate	*Acer, Hedera, Carpinus betulus, Corylus, Quercus deciduous, Fagus, Castanea, Juglans, Tilia, Ulmus, Fraxinus ornus* type
Mediterranean	*Pistacia, Buxus, Quercus ilex, Quercus suber, Olea, Phillyrea, Ostrya carpinifolia, Cistus, Arbutus unedo*
Herbaceous	Apiaceae undiff., Asteroidae, Cichorioideae, *Helianthemum,* Convolvulaceae undiff., Ericaceae undiff., *Erica arborea* type, Lamiaceae undiff., Liliaceae undiff., *Asphodelus,* Plantaginaceae undiff., *Plantago, Plantago lanceolata,* Celastraceae undiff.
Pioneer	Cupressaceae undiff., *Juniperus, Centaurea, Centaurea scabiosa, Centaurea cyanus*
Steppic	*Artemisia,* Chenopodiaceae undiff., *Ephedra distachya, Ephedra fragilis,* Poaceae undiff., *Paronychia/Herniaria, Lygeum*
Ubiquists	Brassicaceae undiff., Gentianaceae, Campanulaceae undiff., Caryophyllaceae undiff., Cistaceae undiff., Dipsacaceae undiff., *Scabiosa, Knautia,* Euphorbiaceae undiff., Fabaceae undiff., Geraniaceae undiff., *Carya, Euonymus,* Ranunculaceae undiff., Rosaceae undiff., Rubiaceae undiff., Saxifragaceae undiff., Solanaceae undiff., Urticaceae undiff.
Aquatics	*Typha/Sparganium*, *Isoetes* type, Cyperaceae undiff., *Thalictrum*, *Nymphaea*

type = plausible taxonomic attribution based on morphology
undiff. = undifferentiated

3.3. Statistical methods

Zonation in the pollen diagram was achieved by using the Constrained Incremental Sum-of-Squares (CONISS) cluster analysis method, based on the TLP. Zone 976-VIII-10 was added manually, based on visual observation of the CONISS results and changes in the pollen assemblage which needed highlighting. To help visualise the results from the pollen analysis, Principal Component Analysis (PCA) was implemented using PAST (Paleontological Statistic) (Hammer *et al.*, 2001). PCA plots show the distribution of samples and the loadings of the ecological groups, achieved by summing the percentages of the taxa in each group (table 2).

4. Results

4.1 Pollen analysis

Pollen analysis on the marine sequence ODP976 produced a high-resolution continuous record spanning the timeframe between 434 and 356 ka BP (MIS 12 to MIS 10), with an average temporal resolution of 480 years. A higher average temporal resolution of 128 years between samples was achieved in the portion representative of the transition MIS 12/11, while the depths representative of the end of MIS 11 and initiation of MIS 10 have a lower resolution of 400 years.

The average TLP count for each sample was 160.8, and only in 6 samples the target of 150 pollen grains was not reached (75–142 grains). The total sum of counted pollen grains for all the samples was 22,680 (not including *Pinus*). The average number of taxa included in the TLP for each sample was 21. In total, 89 pollen taxa were identified. *Pinus* was found to be overrepresented as in many other studies in the region, with a total sum of 42,061 pollen grains for all the samples. Absolute concentrations of land pollen (excluding *Pinus*) have a range of 2,964–76,473 grains/g, with the highest values occurring in two intervals at 116.55–117.08 m and 107.3–110.1 m. Pollen preservation was good throughout the core considering its marine origin, with 0.5–9% of pollen considered indeterminable.

Pollen zonation through CONISS revealed eight palynologically distinctive zones, summarised in Table 3. The percentage pollen diagram in Figure 4 shows taxa with abundances over 5%.

Pollen assemblages show a clear shift from a high abundance of *Pinus*, pioneer and steppic taxa in zone 976-I-12 to an assemblage comprised of temperate and Mediterranean taxa in zone 976-II-11. In zone 976-III-11, *Quercus deciduous* replaces *Pinus* as the dominant taxon and temperate and Mediterranean taxa reach their maximum levels. In zone 976-IV-11, temperate and Mediterranean taxa still represent the dominant proportion of the pollen assemblage, but towards the top of the zone *Q. deciduous* and *Q. ilex* slowly decline while *Artemisia*, *Cedrus* and *Pinus* increase. In zone 976-V-11 there is a shift from temperate and Mediterranean taxa to a higher abundance of *Pinus*, *Cedrus* and steppic taxa. There is a renewed increase in temperate taxa in zone 976-VI-11, but Mediterranean taxa remain low and high abundances of *Pinus* and *Cedrus* persist. From zone 976-VII-11 to 976-VIII-10, there is a continuous decrease in temperate and Mediterranean taxa and an increase in *Pinus*, montane and steppic taxa.

Table 3 – Description of pollen assemblage zones.

Zone	Depth (m)	Age (ka BP)	Pollen description
976-VIII-10	98.85–100.85	356.456–365.343	*Pinus* reaches abundances up to 77%. *Cedrus* is very abundant 22–36%. Decrease in temperate taxa (*Q. deciduous* 4–20%) and Mediterranean taxa appear only sporadically (*Q. ilex* <2%). Herbaceous and pioneer taxa are present at <10%. *Isoetes* spores decrease and disappear at the end of the zone.
976-VII-11	100.85–105.5	365.343–386.005	Increase in *Pinus* (>60%), montane (*Cedrus* >20%) and steppic taxa (Artemisia >10%). Decrease in temperate and Mediterranean taxa. *Q. deciduous* declines (<20%). *Q. ilex* decreases to <4% and other Mediterranean taxa (*Olea*, *Cistus*) decline to <2%. Herbaceous taxa are consistently present, and pioneer taxa (Cupressaceae and *Centaurea*) are present at low rates. *Isoetes* spores decrease to less than 10%.
976-VI-11	105.5–108.95	386.005–399.435	Slight increase in temperate (*Q. deciduous*) and herbaceous taxa (Cichorioideae). Mediterranean taxa remain at very low rates (*Q. ilex*, *Cistus* and *Phillyrea* occur at abundances <5%). *Olea* appears sporadically at abundances <3%. *Pinus* (20–40%), *Cedrus* (15–20%)

			and steppic taxa (*Artemisia*, Chenopodiaceae and *Ephedra*) undergo a slight decline but remain dominant. Cupressaceae occur at rates around 3%. *Isoetes* spores increase, reaching levels around 15%.
976-V-11	108.95–110.03	399.435–403.140	Temperate and Mediterranean taxa decline to half their previous abundance (*Q. deciduous* 10%, *Q. ilex* 2%). All other Mediterranean and temperate taxa decrease to near zero values except for *Cistus* which persists at an abundance of 3-5%. *Pinus* rises to over 60%. Increase in abundance of montane (*Cedrus* 30–40%) and steppic taxa (*Artemisia* 20%). Chenopodiaceae and *Ephedra* also increase. Poaceae remains constantly abundant (10–15%). Herbaceous taxa decrease (Cichorioideae and c.f. *Erica arborea*). *Isoetes* spores decline (<2%).
976-IV-11	110.03–112.11	403.140–410.277	*Q. deciduous* is the most dominant taxon, although it undergoes a steady decline with two significant drops at 111.74m (27%) and 110.28m (23%). *Q. ilex* decreases in this zone (5-11%). *Olea* decreases to an average of 4%. *Cistus* becomes more consistently present (2–6%). *Pinus* abundances remain low (5–15%) but increase slightly towards the top of the zone (23%). Herbaceous taxa become increasingly prevalent (Asteroideae up to 10%, Cichorioideae average 24%). Steppic taxa (Poaceae) are abundant at the beginning of the zone (up to 14%) before decreasing to <10 5% at the top. *Isoetes* spores reach their maximum abundance (17–26%).
976-III-11	112.11–115.89	410.277–423.227	*Q. deciduous* is the most abundant taxon (up to 51%), peaking above 45% at 113.02 m, 112.74 m, 112.26 m and 112.16m. *Q. ilex* also reaches its maximum abundance (peaks >15% at 113.94 m, 113.34 m and 113.02 m). *Olea* abundance is low but continuous (5–8%). Other Mediterranean taxa including *Phillyrea* and *Cistus* occur intermittently. *Pinus* declines to 15–20%. Abundances of riparian taxa are low, with *Salix* representing the most continuous taxon. Pioneer and steppic taxa are low (<10%). *Cedrus* appears intermittently below 2%. Cichorioideae remain abundant (up to 19%). Pioneer taxa abundances are only present sporadically at low abundances, while steppic taxa show continuous abundances. *Isoetes* spores increase (15–20%).
976-II-11	115.89–116.93	423.227–426.648	Temperate and Mediterranean taxa increase rapidly, while the abundances of montane, pioneer and steppic taxa decrease drastically. *Pinus* declines from 52% to 24%, *Cedrus* declines to less than 5%. *Quercus deciduous* increases to 30%. Riparian taxa (*Salix* and *Betula*) are present at low abundances. *Quercus ilex* (4–8%) and *Olea* (6–17%) make up the majority of Mediterranean taxa. Herbaceous taxa are abundant (Cichorioideae 15% and c.f. *Erica arborea* 8%). Cupressaceae decrease to 1–2%, while steppic taxa decline to <10%. *Isoetes* spores increase slightly.
976-I-12	116.93–118.8	426.688–433.868	*Pinus* is abundant (46–86%) with a peak at 118.14 m. *Cedrus* is abundant (up to 17%). *Picea* and *Abies* are present. *Quercus deciduous* is low (< 10%). Mediterranean taxa are mostly absent, except for individual grains of *Phillyrea* and *Cistus*. Herbaceous taxa are prevalent throughout, predominantly Cichorioideae (up to 28%). Pioneer (Cupressaceae 10%) and steppic taxa (*Artemisia* up to 29%, Poaceae 10–30%, *Ephedra distachya* and *Ephedra fragilis* up to 10%) are abundant.

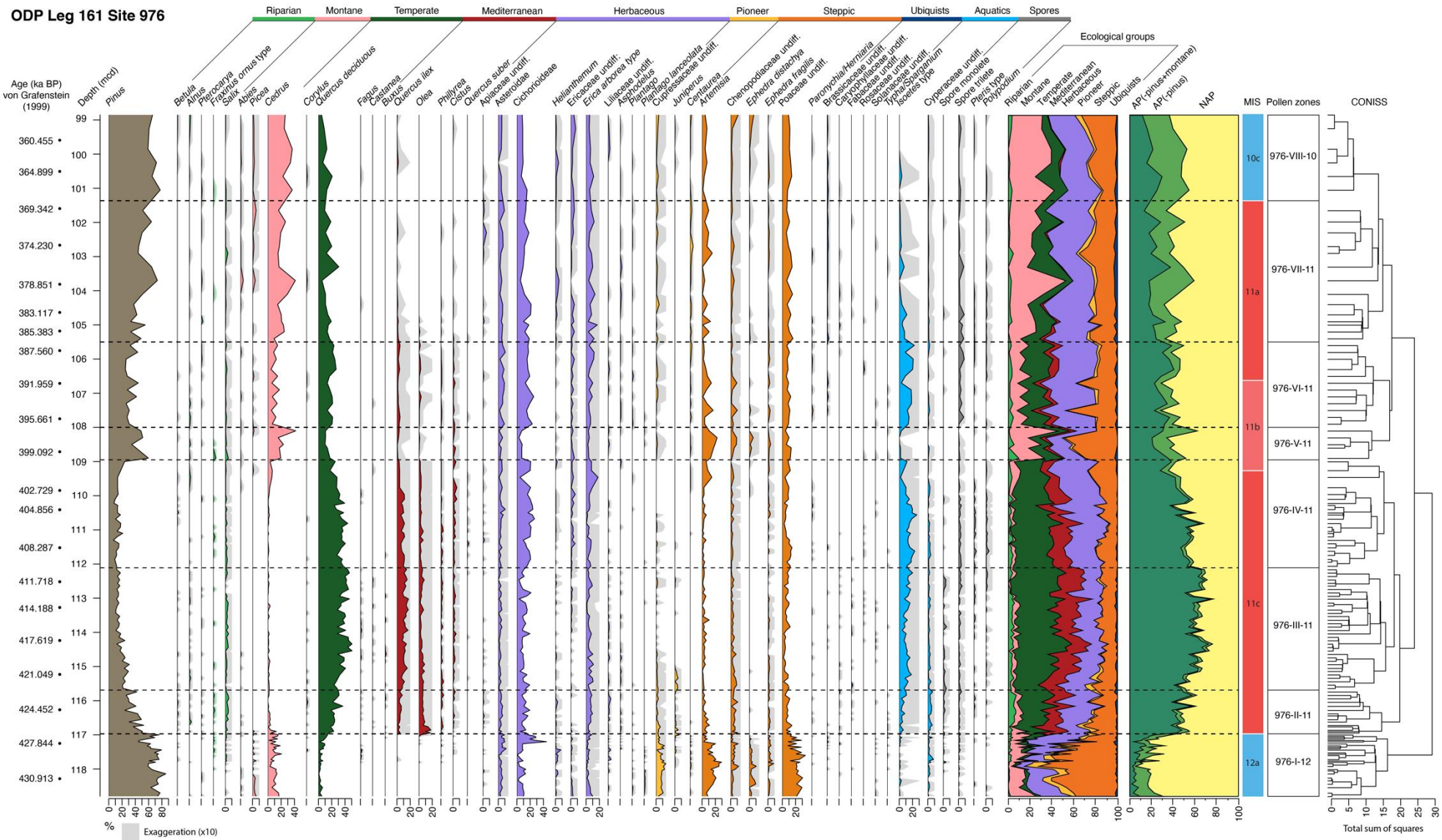

Figure 4 – Pollen percentage diagram for ODP Site 976, showing taxa reaching >5% abundance plotted against depth. On the left, ages (in ka BP) from von Grafenstein *et al.* (1999) are plotted according to meters composite depth (mcd). Synthetic diagrams showing the ecological groups and AP/NAP pollen curves are shown on the right. Pollen zones with CONISS clusteirng, and MIS stage equivalents, are shown on the far right. Data for taxa <5% is available in the supplementary data. Grey curves in the background indicate the x10 exaggeration.

4.2 PCA analysis

PCA of the ecological groups, excluding *Pinus*, aquatics and spores (Fig. 5A), found that PC1 represents 64% of the total variance while PC2 represents 20%. Samples appear to be broadly clustered according to the zonation produced through CONISS. Zones 976-I-12, 976-VI-11, 976-VII-11 and 976-VIII-10 are primarily found on the left of the biplot with negative values in PC1, and their variance is also represented in PC2 with scores ranging from -30 to 30. These samples appear to be influenced mainly by montane (*Cedrus*, *Picea*), steppic (*Juniperus*, Poaceae, Cupressaceae) and pioneer groups (*Artemisia*). Zone 976-II-11 is clustered close to the centre of the PCA plot, and seems to be influenced primarily by the riparian and pioneer taxa (mainly *Ephedra distachya*, Chenopodiaceae and Cupressaceae). Zones 976-III-11, 976-IV-11 and 976-V-11 are mostly clustered to the left of the diagram with primarily negative scores in PC1 and are limited within a range of -7.5–7.5 in PC2. These zones appear to be primarily influenced by temperate and Mediterranean groups (*Q. deciduous*, *Q. ilex*, *Cistus* and *Olea*).

A more focused PCA was also run on the samples from zones 976-II-11 to 976-VII-11 assumed to represent the MIS 11 interglacial (Fig. 5B), achieved by removing zones significantly influenced by montane and steppic taxa (976-I-12 and 976-VIII-10). In this plot, PC1 represents 59% of the total variance while PC2 represents 18%. The clustering of the samples reveals significant differences between these zones. Zone 976-II-11 remains distributed around the middle of the biplot, with predominantly negative scores in PC2 and influenced by pioneer, riparian and steppic taxa. Zone 976-V-11 also is distributed closer to the centre of the plot, but appears to be more influenced by herbaceous taxa and has more positive scores in PC2. Zones 976-III-11 and 976-IV-11 are clustered on the right, although zone 976-III-11 is predominantly influenced by temperate and Mediterranean taxa while zone 976-IV-11 is more influenced by ubiquist taxa. Meanwhile, zones 976-VI-11 and VII are distributed to the left and are similarly influenced by herbaceous and montane groups, although zone 976-VII-11 has overall more negative scores in PC1.

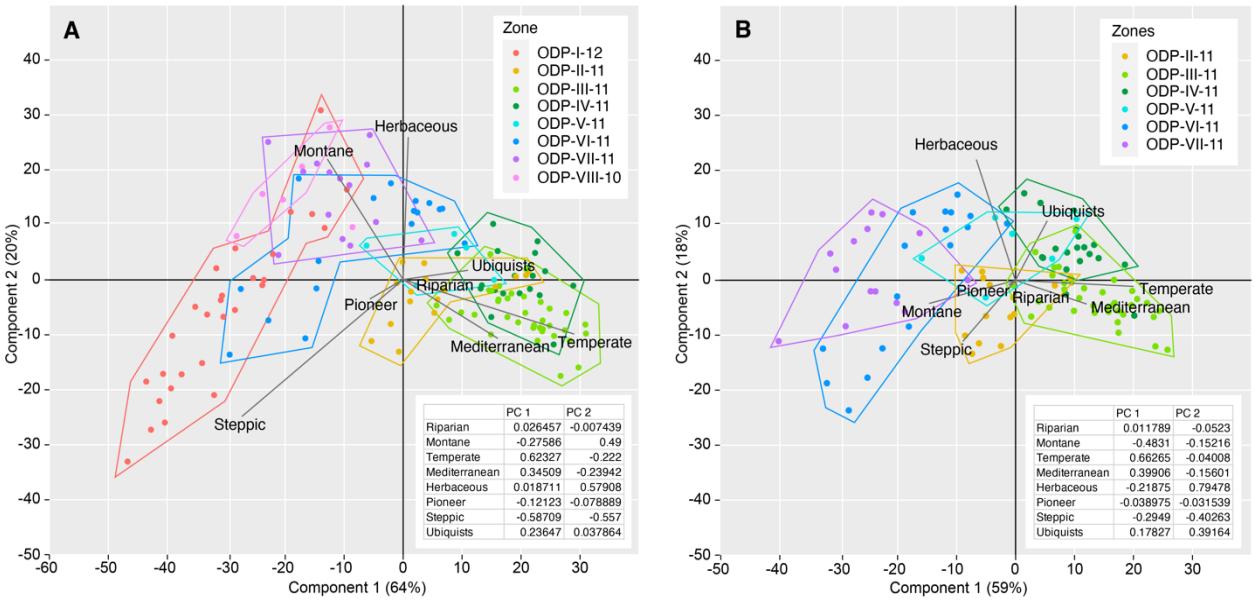

Figure 5 – Principal Component Analyses (PCA) of samples from (A) the entire record and (B) samples only from zones 976-II-11 to 976-VII-11, showing their distribution in relation to ecological groups. *Pinus*, aquatics and spores have been omitted from the analysis. Loadings of the ecological groups for PC1 and PC2 are presented in the bottom right of each plot.

5. Discussion

5.1 Palaeoenvironmental interpretations

Pollen results in the lowermost zone of this record (976-I-12), representing the period between 434 and 427 ka BP, show that the assemblage is dominated by *Pinus,* high abundances of steppic and pioneer taxa such as Poaceae, Cupressaceae, *Artemisia*, *E. distachya* and *E. fragilis*, suggesting that a cold climate prevailed in the region consistent with the MIS 12 glacial period. These conditions would have limited the establishment of temperate trees leaving a semi-desertic landscape characterised mainly by shrubs at the lower altitudes of the Mediterranean (Hes *et al.*, 2022). At mid- and higher altitudes, *Pinus* and other montane taxa (mainly conifers, i.e. *Cedrus* and *Picea*) would have prevailed.

An abrupt climatic shift is observed between zones 976-I-12 and 976-II-11, in which *Pinus,* montane, pioneer and steppic decrease drastically and are replaced by arboreal associations composed of riparian, temperate and Mediterranean taxa (Fig. 6A). This is a clear indication of the transition between MIS 12 and 11, observed specifically around 426 ka BP. The onset of assemblages comprised of *Salix*, *Quercus deciduous*, *Q. ilex* and *Olea* suggests a rapid climatic amelioration towards a warmer and more humid setting. Particularly, the marked rise in *Olea* at this time, a genus typical of the thermo-Mediterranean belt and commonly associated with warm interglacials of the Pleistocene and Holocene (Punt and Blackmore, 1991; Quézel and Medail, 2003), is indicative of a significant rise in temperatures. Furthermore, the gradual increase in *Isoetes*, a taxon which is related to marshlands and freshwater, is suggestive of higher precipitation associated with the transition from glacial to interglacial (Sánchez Goñi *et al.*, 1999). The amplitude of the transition observed in this record is in line with the overall consensus that Termination V represents an extreme climatic shift (Droxler *et al.*, 2003).

The expansion of the temperate and Mediterranean forest in zones 976-III-11 and IV, and the consistently low percentages of *Pinus,* pioneer and steppic taxa, correspond to the period between 423 and 403 ka BP which can be correlated with the long and warm climatic optimum MIS 11c. The results are consistent with intense warmth and elevated humidity also recognised in other terrestrial and marine Mediterranean records (Oliveira *et al.*, 2016; Kousis *et al.*, 2018; Azibeiro *et al.*, 2021). Specifically, the period represented by zone 976-III-11 (423–410 ka BP) exhibits the highest abundance of temperate and Mediterranean taxa in the entire record, an assemblage made up mostly of *Q. deciduous*, *Q. ilex*, *Olea*, *Phillyrea* and *Cistus* occurring along a continuous high abundance of *Isoetes*. This period represents the warmest phase recorded, consistent with the MIS 11c climatic optimum. This is followed by a gradual decline in temperate and Mediterranean taxa throughout zone 976-IV-11, representing the latter part of MIS 11c (410–403 ka BP). Although in decline, the temperate forest still represents the dominant proportion of the assemblage and the rates of *Q. ilex* are still relatively high compared to the previous zone. Combined with the high abundances of *Isoetes* and the low rates of pioneer and steppic taxa, this indicates that the climate was predominantly warm and wet.

The slowly decreasing trends of *Q. deciduous* and Mediterranean taxa and the increase in *Pinus* and *Cedrus* towards the upper part of zone 976-IV-11, around ca. 400 ka BP, may indicate the onset of a cooler phase recognised in other studies as MIS 11b (Desprat *et al.*, 2006; Oliveira *et al.*, 2016; Kousis *et al.*, 2018; Ardenghi *et al.*, 2019). In zone 976-V-11, the shift observed from temperate and Mediterranean taxa to an assemblage comprising *Pinus*, *Cedrus*, and steppic taxa (*Artemisia*, Chenopodiaceae, *E. distachya* and *E. fragilis*) is indicative of a decline in temperature and an increase in aridity. The persistence of *Q. deciduous* and

some Mediterranean taxa (e.g. *Q. ilex*, *Olea*, *Cistus*, although at abundances <3%) suggest that the climate was still viable for the presence of humid forests, but not warm or moist enough to support the high forest cover seen during the optimum, leading to a significant forest contraction. The expansion of *Cedrus* at mid-altitude, the increase of *Artemisia* and the decline of *Isoetes* are particularly indicative of a drier climate which would have been too harsh for temperate and Mediterranean trees, leading to colonisation by conifers and shrubs typical of a cool period.

This cooler phase is followed by a renewed increase in temperate taxa and a minimal rise in Mediterranean taxa, observed in zone 976-VII-11, indicating a new period of forest expansion. Together with the increase in *Isoetes*, this may be interpreted as a return of warm and humid conditions suitable for the expansion of a temperate forest, albeit reduced compared to the climatic optimum as suggested by the persistently higher abundances of *Pinus*, *Cedrus* and *Artemisia*. This phase is consistent with the conditions of MIS 11a, which is often recognised as a period of transition from temperate deciduous to cold mixed forests (Kousis *et al.*, 2018) indicative of high climatic variability (Candy *et al.*, 2014).

The uppermost zones, 976-VII-11 and VIII-10 (386–356 ka BP), encompass the transition from MIS 11 to the glacial MIS 10. The end of MIS 11a is characterised by large fluctuations in the temperate and montane forests, with a particular phase of contraction in *Q. deciduous* and an expansion of *Pinus* and *Cedrus* around 380 ka BP. This particular event occurs without an increase of steppic and pioneer taxa suggesting that a semi-arid shrubland did not develop and therefore this was a predominantly cold event not subject to a change in humidity. Such an increase in conifers, especially *Cedrus*, without a particular increase in semi-desert taxa, may also signify a probably enhanced wind input from the south of the Alboran Sea associated with the settling of montane forests in the high-altitudes of the Betic and Rif Arc mountains (Magri and Parra, 2002; Bout-Roumazeille *et al.*, 2007; Combourieu-Nebout *et al.*, 2009). This period is followed in zone 976-VIII-10 by a steady decline in *Q. deciduous* and a very sporadic appearance of Mediterranean taxa, consistent with the long-term cooling trend towards MIS 10 (McManus *et al.*, 2003; Oliveira *et al.*, 2016). *Pinus* and *Cedrus* become the dominant taxa, accompanied by a rise in Cupressaceae, Chenopodiaceae and *E. distachya,* which is interpreted as the return of glacial conditions at the onset of MIS 10 around 367 ka BP, characterised by a predominantly montane forest and herbaceous/steppic assemblages.

5.2 MIS 12/11 transition

The shift in vegetation recorded in ODP976 between 430 and 425 ka BP, characterised by the sharp transition from *Pinus,* montane and steppic taxa to temperate and Mediterranean assemblages, represents the period of climatic change from the cold and arid conditions of MIS 12 to the warm and humid conditions of MIS 11. This transition has been documented in several palaeoenvironmental and palaeoclimatic records from the Mediterranean (Tzedakis *et al.*, 2001; Girone *et al.*, 2013; Kousis *et al.*, 2018; Ardenghi *et al.*, 2019; Azibeiro *et al.*, 2021), the North Atlantic off the Iberian coast (Desprat *et al.*, 2005; Oliveira *et al.*, 2016) and continental Europe (Reille and de Beaulieu, 1995). The timing of the transition is largely synchronous across the records in the Mediterranean and North Atlantic and has been identified between 428 and 424 ka BP (Figs. 6 and 7).

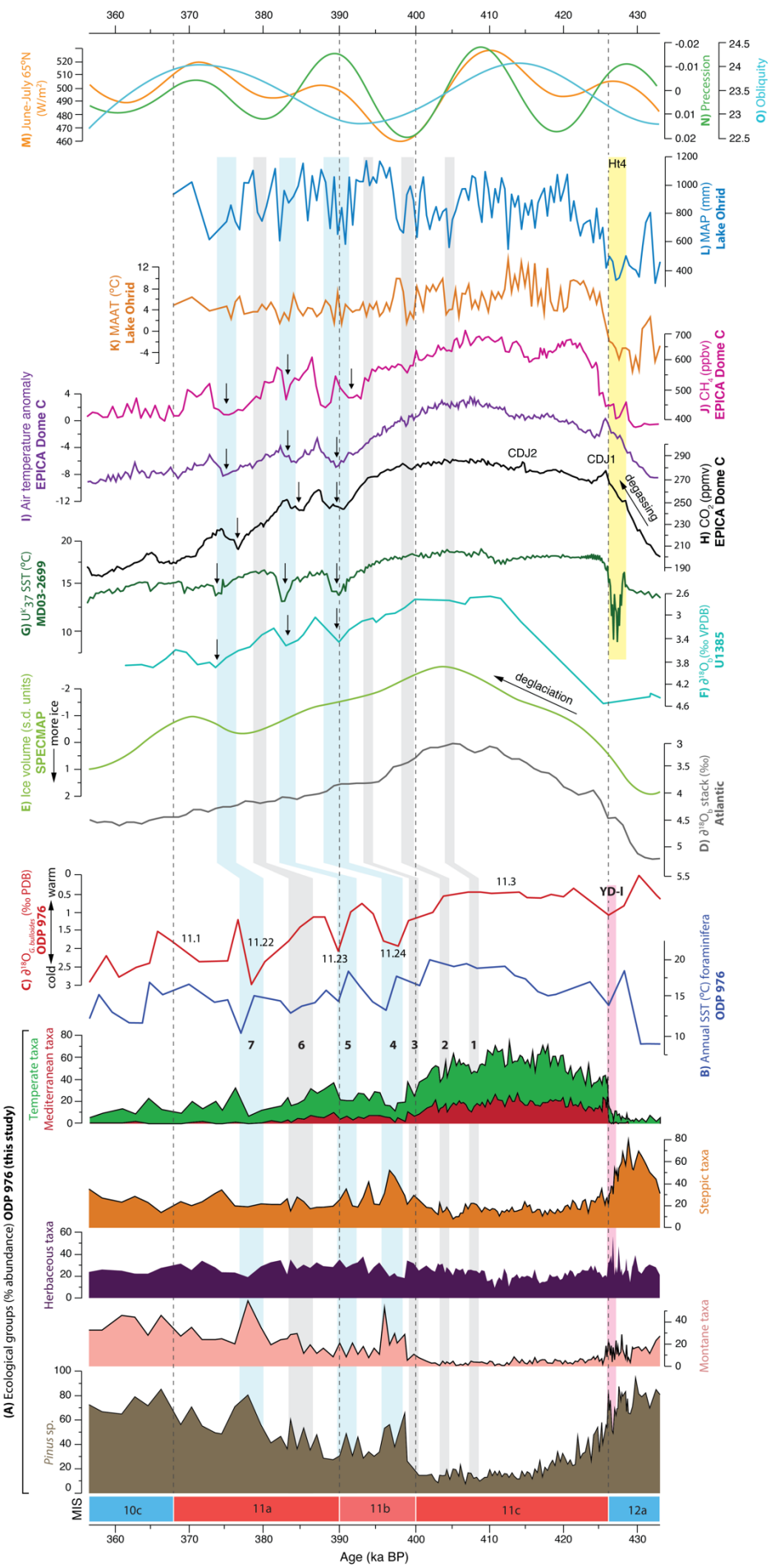

Figure 6 – *Comparison between (A) selected ecological groups from the ODP Site 976 record in this study, and proxies of climatic variability: (B) Annual SSTs from function transfer of foraminiferal assemblages and (C) $\delta^{18}O_{G.\ bulloides}$ from ODP Site 976 (Brice, 2007), with numbered light and heavy isotopic events after Bassinot et al. (1994); (D) Benthic $\delta^{18}O$ stack from the Atlantic (Lisiecki and Raymo, 2009); (E) Ice volume from SPECMAP stacked $\delta^{18}O$ (Imbrie et al, 1984); (F) Benthic $\delta^{18}O$ from U1385 (Oliveira et al., 2016); (G) Alkenone SSTs from MD03-2699 (Rodrigues et al., 2011); (H) CO_2 atmospheric concentrations from Antarctic EPICA Dome C ice core (Nehrbass-Ahles et al., 2020); (I) Antarctic air temperature anomaly from Antarctic EPICA Dome C ice core (Jouzel et al., 2007); (J) Methane (CH_4) atmospheric concentrations from Antarctic ice cores EDC (Loulergue et al., 2008); (K) Mean annual temperature and (L) Mean annual precipitation reconstructions from Lake Ohrid (Kousis et al., 2018); (M) Summer insolation (Laskar et al., 2004); (N) Precession index and (O) Obliquity curve (Berger and Loutre, 1991). All curves are plotted within their original chronological framework. Numbered bands indicate millennial-scale forest contractions of high (blue bands 4, 5 and 7) and moderate intensity (grey bands 1, 2, 3 and 6). The light pink band indicates the Younger Dryas-like event, while the yellow band highlights the Ht4 event observed in other records.*

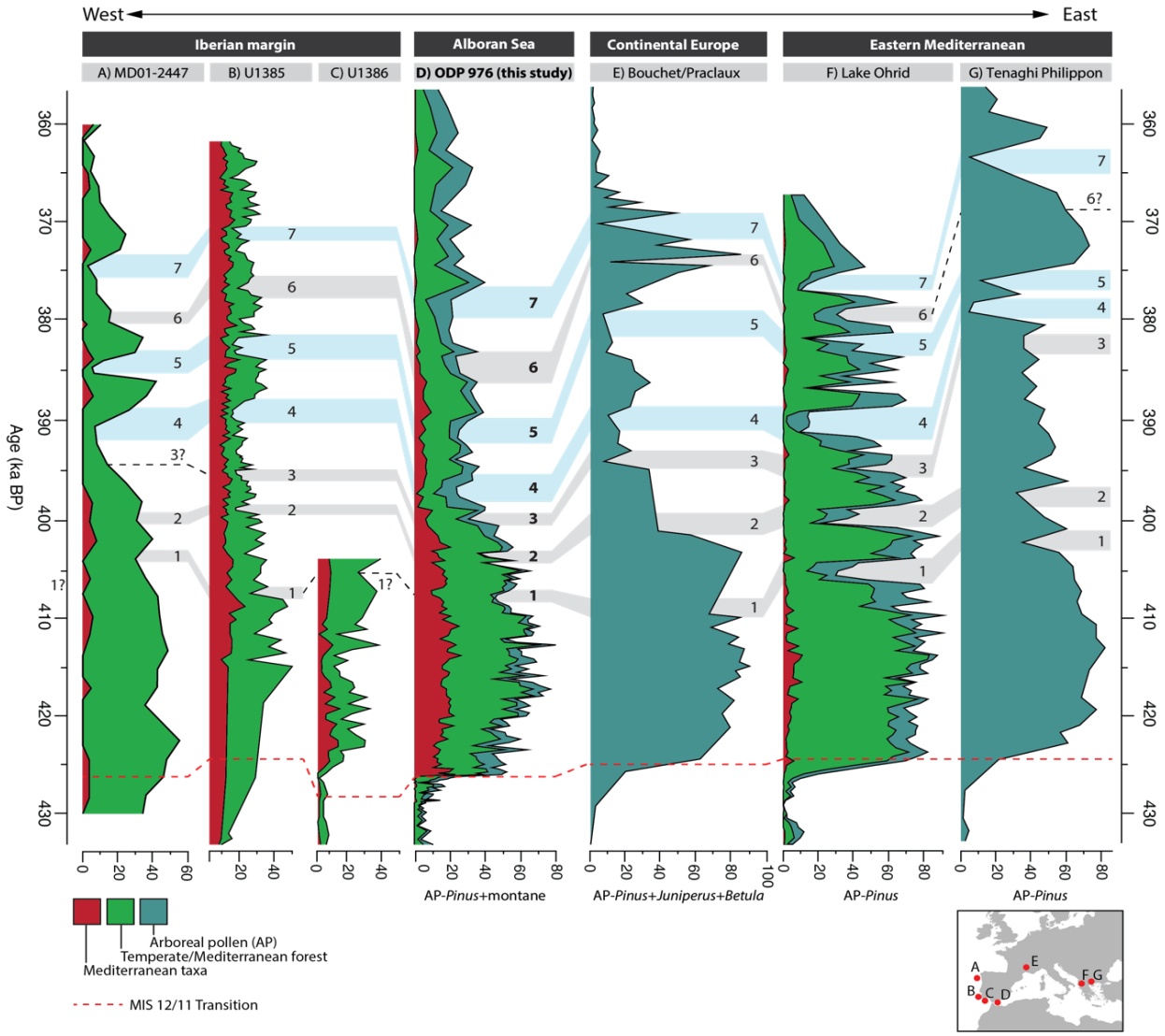

Figure 7 – Comparison of the AP curves and the Mediterranean and temperate ecological groups of high-resolution pollen records from the Mediterranean which encompass MIS 12 and 11: (A) Marine site MD01-2447 (Desprat *et al.*, 2005); (B) Marine site IDOP U1385 (Oliveira *et al.*, 2016); (C) Marine site IODP U1386 (Hes *et al.*, 2022); (D) Marine site ODP 976 (this study); (E) Bouchet/Praclaux (drawn after Reille and de Beaulieu, 1995); (F) Lake Ohrid (Kousis *et al.*, 2018); (G) Tenaghi Philippon (Ardenghi *et al.*, 2019). Coloured bands indicate the millennial-scale forest contraction events identified in Figure 6, and the tentative correlations made with the other records. Dotted line indicates a correlation where no analogue was identified. All records are plotted within their original chronological framework.

The changes observed in our pollen record coincide with independent Sea Surface Temperature (SST) reconstructions and planktonic $\delta^{18}O_{Globigerina\ bulloides}$ records derived from ODP976 (Fig. 6B and C) by Brice (2007), which show an overall increase from around 9 to 17°C between 432 and 427 ka BP, and a drop in $\delta^{18}O$ values from 1 to nearly 0‰ around 430 ka BP (Brice, 2007). This decrease in $\delta^{18}O_{G.\ bulloides}$ and the associated rise in SSTs were also detected in several other marine records from the North Atlantic and Iberian Margin (e.g. Jouzel *et al.*, 2007; Voelker *et al.*, 2010; Vázquez Riveiros *et al.*, 2013; Oliveira *et al.*, 2016) as well as in the Mediterranean at sites ODP 975 (Girone *et al.*, 2013) and ODP 977 (Azibeiro *et al.*, 2021), showing a coeval response of these regions to global climatic change. Specifically, this trend is indicative of the inflow of meltwater from the North Atlantic into the Strait of Gibraltar as a result of the decrease in ice volume caused by increasing insolation (Hes *et al.*, 2022; Candy

et al., 2014), as corroborated by the SPECMAP isotopic stack record (Fig. 6E) (Bassinot *et al.*, 1994; Imbrie *et al.*, 1984).

This trend of climatic amelioration is interrupted by an abrupt return to colder and drier conditions around 428–426 ka BP as evidenced by the sudden decrease SSTs and an episode of rapid increase in $\delta^{18}O_{G.\ bulloides}$ (Brice, 2007), which corresponds with a coeval and short-lived increase in *Pinus*, montane taxa and herbaceous taxa (Cichorioideae) at the expense of temperate taxa at 427 ka BP, at the interface between MIS 12 and 11 (Fig. 6). Brice (2007) defines this interval as a Younger Dryas-like event (YD-I), given its resemblance to the event following the last deglaciation between 12.9 and 11.5 ka BP. Other studies have identified a prominent cold phase during the transition, and have sometimes referred to as Heinrich-type event Ht4 (Hodell *et al.*, 2008; Rodrigues *et al.*, 2011; Girone *et al.*, 2013; Marino *et al.*, 2018). Vázquez Riveiros *et al.* (2013) observed a pulse of enhanced Ice Rafted Debris (IRD) in their record from ODP980 between 430 and 425 ka BP, synchronous with a sharp reduction in North Atlantic SSTs, suggesting a substantial ice-rafting event accompanied by a large production of brine waters during this time. This phase was also recorded by Rodrigues *et al.* (2011) in their alkenone-derived SST record from core MD03-2699 (Fig. 6G) and by Regattieri *et al.* (2016) in their $\delta^{18}O$ record from the Sulmona basin in central Italy, showing similar responses in marine and terrestrial records. These events are common in many North Atlantic records (e.g. McManus *et al.*, 1999; Voelker *et al.*, 2010) and are related to major ice-sheet instability during periods of climate reorganisation (Regattieri *et al.*, 2016). This phase is also corroborated by the pollen-based reconstructions by Kousis *et al.* (2018) for Lake Ohrid which show a decrease in mean annual atmospheric temperatures (MAAT; Fig. 6K) and mean annual precipitation (MAP; Fig. 6L), and a phase of reduced forest cover in their pollen record at this site between 430 and 427 ka BP (Fig. 7). However, while the Ht4 stadial recognised in other records is generally understood as a cold and dry event, the peak of Cichorioideae in our record leads to the interpretation of a cold but rather humid event in this part of the Mediterranean. As suggested by several authors (e.g. Vázquez Riveiros *et al.*, 2013; Tzedakis *et al.*, 2022), the influx of freshwater caused by the deglaciation led to a weakening of the Atlantic Meridional Overturning Circulation (AMOC), which may have been caused by the activation of a bipolar see-saw pattern in precipitation between the western and eastern Mediterranean.

The YD-I/Ht4 event decreased the cooling effect of cold water upwelling as a result of the weakened AMOC, in turn leading to the further warming of Antarctica (Tzedakis *et al.*, 2022). This is visible in panels H, I and J in Figure 6, which show the steady increase in the CO_2, air temperature and methane (CH_4) records from the Antarctic EPICA Dome C ice cores (Jouzel *et al.*, 2007; Loulergue *et al.*, 2008; Nehrbass-Ahles *et al.*, 2020). This exceptional warming and increase in greenhouse gas concentrations may explain the high biosphere productivity and the major increase in global forest biomass during Termination V (Brandon *et al.*, 2020). Among the pollen records from the Mediterranean and continental Europe, the onset of MIS 11c is represented by a pronounced phase of forest expansion (Fig. 7). Though the specific timing of this increase in forest cover is slightly different, possibly due to discrepancies between chronologies, this response is likely to have been caused by a large uptake of atmospheric CO_2 during the degassing period (Tzedakis *et al.*, 2022). The peak in CO_2 at 426 ka BP—also known as the first 'Carbon Dioxide Jump' (CDJ) (Tzedakis *et al.*, 2022)—and the concomitant peak in Antarctic air temperatures, are particularly important as they correlate with the dramatic rise in *Olea* and *Q. ilex* at this time in the ODP976 record. This interpretation is in agreement with pollen-based climatic reconstructions from Lake Ohrid, which suggest a

transition towards wetter and warmer conditions at the onset of MIS 11c, evidenced by a rise in MAAT by 7°C and in MAP by 150 mm at Lake Ohrid (Kousis *et al.*, 2018). The development of more Mediterranean conditions around the lower latitudes of the Alboran Sea during this time would have been necessary for the expansion of evergreen forests (Okuda *et al.*, 2001).

Regionally, our results are in agreement with palynological records from Lake Ohrid (Kousis *et al.*, 2018), Tenaghi Philippon (Wijmstra and Smit, 1976; Tzedakis *et al.*, 2006; Ardenghi *et al.*, 2019) and Bouchet/Praclaux (Reille and de Beaulieu, 1995), which show a synchronous expansion of forest biomass throughout Termination V. This overall trend is corroborated by palaeoclimatic data from the North Atlantic and Mediterranean which record increasing SSTs, CO_2, CH_4 and a significant drop in $\delta^{18}O$. These patterns are significant because they demonstrate analogous changes in vegetation in terrestrial and marine records during this period. Nevertheless, a close comparison with the high-resolution pollen record of Lake Ohrid reveals that the amplitude of change in Mediterranean vegetation at ODP976 during the MIS 12/11 transition is significantly greater. This could suggest that the ODP976 record reflects a warmer and drier climate at the onset of MIS 11c in the southwestern Mediterranean compared to the Balkan Peninsula where Lake Ohrid is located. Due to the higher altitude of Lake Ohrid (1514 m asl) and its geomorphological context, however, this site may be recording a more local signal from a subdued Mediterranean forest, while the ODP976 marine record is likely to represent a wider regional signal of the vegetation changes occurring around the Alboran sea.

5. 3 MIS 11 vegetation and climatic variability

5.3.1 Long-term vegetation and climate change

Evaluation of the pollen data indicates that MIS 11c was the warmest substage, characterised by the maximum forest extent consistent with a climatic optimum between 426–400 ka BP, observed ubiquitously across palaeoenvironmental and palaeoclimatic records. This substage is often characterised by the largest expansion of mixed oak forest and Mediterranean taxa (Fig. 6), concurrent with the results from ODP976. This forest expansion, also referred to as the 'Sines' forest phase in marine records from the Iberian margin (Oliveira *et al.*, 2016; Hes *et al.,* 2022), reflects the highest degree of warming and seasonal rainfall in the south-western Mediterranean, and is associated with the light isotopic event MIS 11.3 (see Fig. 6C) as well as the strongest Northern Hemisphere summer insolation of the interglacial (Fig. 6M) (Oliveira *et al.*, 2016). The occurrence of warm conditions is particularly supported by the presence of thermophilous taxa such as *Q. ilex*, *Phillyrea* and *Olea*, which require warm and dry summers and mild winters (San-Miguel-Ayanz *et al.*, 2016). Similar findings were reported by Kousis *et al.* (2018) at Lake Ohrid for this period, who showed that annual temperatures for their site reached up to 9.5°C between 415 and 412 ka BP, with mean temperatures for the coldest month (MTCO) around 1.5°C, signifying frost-free winters. Our palaeoenvironmental interpretations correlate well with the highest foraminifera- and alkenone-based SSTs, maximum concentrations of CO_2 and CH_4 from the EPICA ice cores (Jouzel *et al.*, 2007; Nehrbass-Ahles *et al.*, 2020), and diminished $\delta^{18}O$ (e.g. Voelker *et al.*, 2010; Oliveira *et al.*, 2016). However, the ODP976 record appears to be subject to a temporal offset from the end of MIS 11c onwards, most possibly caused by differences in dating methods and the development of more precise chronologies in recent years compared to what we have adopted from von Grafenstein *et al.* (1999). Thus, the climatic optimum observed at OPD976 appears shorter than in tuned records where it is usually observed between ~426 and 396 ka BP (Tzedakis *et al.*, 2022). Nevertheless, our record is in agreement

with most proxies which show that the duration of MIS 11c averaged around 30 ka (McManus *et al.*, 2003; Tzedakis *et al.*, 2022), and the vegetation signatures are comparable with other pollen records from the region.

The exceptional amplitude of response by the temperate and Mediterranean forests to climatic amelioration observed at ODP976 perpetuates the ongoing debate regarding the 'Stage-11 problem' or the 'MIS 11 Paradox' (Imbrie *et al.*, 1984; McManus *et al.*, 2003) which refers to the disparity between the strong environmental and climatic response to the weak insolation forcing during this interglacial (Berger and Wefer, 2003). According to Tzedakis *et al.* (2022), the deglaciation during Termination V was significantly prolonged in comparison to other interglacials, as a result of the weak eccentricity-precession forcing and antiphasing between precession (Fig. 6N) and obliquity (Fig. 6O)—i.e. the occurrence of two precession (and insolation) peaks over the course of one obliquity cycle (Tzedakis *et al.*, 2022). This would have protracted the conditions of the interglacial for a period significantly longer than any subsequent interglacial, leading to a rise in summer insolation at both polar regions thereby enhancing the melting of sea ice and allowing more CO_2 outgassing from the North and South Atlantic (Vázquez Riveiros *et al.*, 2013; Tzedakis *et al.*, 2022).

The abundances of temperate and Mediterranean taxa reach a maximum between 420 and 415 ka BP and remain elevated, in our record, until 410 ka BP, after which they begin to decrease. The long-term forest decline at the end of MIS 11c has also been recorded in other pollen records (Fig. 7) and has been connected to a decrease in summer insolation, showing a regional response of vegetation to solar forcing. These trends also resemble the decline in atmospheric CO_2 and CH_4 records from Antarctica (Jouzel *et al.*, 2007; Loulergue *et al.*, 2008) and the decline in alkenone-based SSTs from the North Atlantic between 415 and 390 ka BP (Fig. 6).

The pollen data in the record ODP976 suggests an overall cooling during substage MIS 11b (400–390 ka BP) and a return of relatively warmer conditions during MIS 11a (390–367 ka BP), though reduced compared to MIS 11c, inferred from the large fluctuations between temperate and montane forests which suggest significant variability in aridity and temperature. These changes are in agreement with the patterns observed in many other palaeoclimatic and palynological records from the North Atlantic and Mediterranean (Candy *et al*., 2014) and appear to closely follow changes in summer insolation and can be correlated with light isotopic events recognised in $\delta^{18}O$ records (Fig. 6D, E and F), namely 11.24, 11.23 and 11.22 (Desprat *et al.*, 2005; Oliveira *et al.*, 2016). Despite the chronological offset with other records, the pollen data from ODP976 seems to follow insolation and precession cycles more closely than other proxies at other sites. For instance, the increase in *Pinus* and montane taxa during MIS 11b at the expense of temperate and Mediterranean taxa coincides with the insolation and precession minima at 400 ka BP. This supports the idea that, owing to its position in the WAG (see section 2), site ODP976 is sensitive to changes in polar tropical and Atlantic influences caused by climatic variability, and is also a great candidate to observe the influence of the moderate solar forcing of MIS 11 on vegetation.

5.3.2 Millennial-scale vegetation and climatic variability

Following the prolonged and exceptionally stable climatic optimum of MIS 11c, the late part of MIS 11 is characterised by significant millennial-scale oscillations. Previous studies have connected these events with changes in the position of the polar front and the distribution of pressure systems over the North Atlantic during MIS 11 (e.g. Desprat *et al.*, 2007; Oliveira *et al.*, 2018, 2016; Sánchez Goñi *et al.*, 2018; Kousis *et al.*, 2018). Two types of such oscillations

have been identified: 1) moderate events characterised by distinct declines in forest cover with no counterpart in the SST profiles, and (2) high-intensity events marked by contractions in the temperate and Mediterranean forest synchronous with drops in SSTs and annual atmospheric temperatures (Oliveira *et al.*, 2016; Kousis *et al.*, 2018). Our pollen data documented seven of such pronounced forest contractions (marked by the numbered bands in Figs. 6 and 7), and an attempt has been made to tentatively correlate them with the changes observed in other records from the Mediterranean and North Atlantic (Fig. 7).

Four of such moderate-intensity fluctuations in temperate and Mediterranean forest abundance have been identified in our record (grey bands) at ca. 408, 404, 400 and 385 ka BP (events 1, 2, 3 and 6, respectively). The most notable of these oscillations is the first forest contraction, which marks the end of the MIS 11c climatic optimum and has been identified in other pollen records from the region at IODP Site U1385 at 408 ka BP (event U1385-11-fe1; Oliveira *et al.*, 2016), Site MD01-2443 at 406 ka BP (Tzedakis *et al.*, 2009), and at Lake Ohrid between 406.2–404.5 ka BP (event LO-11-1; Kousis *et al.*, 2018). Although it is difficult to locate an equivalent event at the lower-resolution pollen records from Bouchet/Praclaux (Reille and de Beaulieu, 1995) and Tenaghi Philippon (Tzedakis *et al.* 2009) they can be roughly correlated with drops in arboreal pollen around 408 and 402 ka BP, respectively.

Oliveira *et al.* (2016) and Kousis *et al.* (2018) have correlated this first forest contraction with the "Older Holstenian Oscillation" (OHO) detected in records from Germany, Denmark, Poland and Britain (West, 1956; Kelly, 1964; Turner, 1970; Kukla, 2003; Koutsodendris *et al.*, 2011, 2012; Tye et al 2016). During the OHO, vegetation in western and northern Europe underwent similar changes observed at ODP976, characterised by a strong decline in *Quercus* and *Alnus.* These taxa can tolerate cold conditions but require warm summer and spring (Dahl, 1998), thus indicating in the record a reduction in the temperatures of the warmest months. It is thought that the triggering mechanisms of the OHO were similar to the 8.2 ka event during the Holocene, which was driven by a slowdown of the North Atlantic Deep Water (NADW) formation as a result of increased discharges of meltwater from the Laurentide lakes into the North Atlantic (Barber *et al.*, 1999; Ellison *et al.*, 2006). Climate reconstructions from Lake Ohrid estimate a decrease in MAAT from 8 to 4°C and in MAP from 960 to 550 mm (Kousis *et al.*, 2018). Suggestions regarding the duration of a colder and drier climate during the OHO range between 300 and 780 years (Mangili *et al.*, 2007; Tzedakis *et al.*, 2009). Although its timing is debated (Koutsodendris *et al.*, 2010, 2011, 2012), the detection of a similar contraction in temperate forests in other records at a similar time despite chronological discrepancies points towards a synchronous supraregional response to the OHO and therefore we propose an equivalent interpretation for the changes observed in the ODP976 pollen data.

The high-intensity cooling events identified in our record (events 4, 5, 7) are denoted by very pronounced contractions in the temperate and Mediterranean groups and marked increases in *Pinus*, *Cedrus* and steppic taxa. These major cooling events are recognised during MIS 11b and 11a around ca. 397, 390 and 378 ka BP and are synchronous with the three light-isotopic events (11.24, 11.23 and 11.22, respectively) documented by Brice (2007) for ODP976 (Fig. 6C). Despite chronological incongruities, equivalent vegetation responses correlated with abrupt changes in isotopic signatures have been reported by Oliveira *et al.* (2016) at IODP Site U1385 (Fig. 6F and 7B) at ca. 390 (U1385-11-fe5), 383 (U1385-11-fe6) and 371.5 ka BP (U1385-11-fe10), interpreted as indicative of the coolest and driest atmospheric conditions of MIS 11. Similar high-intensity forest contractions have also been documented at MD01-2447 around ca. 392, 383 and 375 ka BP (Desprat *et al.*, 2005, 2007), at Lake Ohrid around

390 (LO-11-4), 382 (LO-11-5) and 377 ka BP (LO-11-7; Kousis *et al.*, 2018), and at Tenaghi Philippon at 384, 378 and 376 ka BP (Ardenghi *et al.,* 2019). Across all records, the strongest forest contraction appears to be related to the first light-isotopic event 11.24 (event 4 in ODP976 at 397 ka BP) which, as indicated by the marked rise in steppic taxa in our record, appears to be the driest and coolest episode of MIS 11. The other two major forest contractions, synchronous with events 11.23 and 11.22, do not occur alongside a substantial rise in steppic assemblages, indicating that they were predominantly cold events not subject to changes in aridity but still caused a significant strain on temperate oak forests.

These high-intensity events have been linked to changes in the AMOC caused by iceberg discharges into the North Atlantic which amplified the cooling process at the end of MIS 11 (Oppo *et al.*, 1998; Martrat *et al.*, 2007; Voelker *et al.*, 2010). Concurrent with the three light-isotopic events, Rodrigues *et al.* (2011) show distinctive reductions to ~10°C in their alkenone-based SST record from MD03-2699 (fig. 6E). Similarly, climatic reconstructions from Lake Ohrid show significant drops in MAAT from 8 to 2°C, and reductions in MAP from around 1000 to 600mm, demonstrating coeval cooling on land as well as the sea-surface during these events which match the changes in assemblages in our ODP976 record. A parallelism can also be made with the sudden drops in atmospheric CO_2 and CH_4 concentrations and air temperature anomalies from the Antarctic EPICA records (Figs. 6I, J and K) which demonstrate the response of vegetation in the Mediterranean to global-scale climate change.

Some authors (Kandiano *et al.*, 2012; Kousis *et al.*, 2018) proposed that drier conditions prevailed in the western Mediterranean and north-western Africa during the millennial-scale climatic events of MIS 11, while wetter conditions occurred in the Balkans, due to the development of a see-saw pattern in precipitation between the western and eastern Mediterranean. While latitudinal and altitudinal differences between sites must be taken into consideration with regard to the climatic reconstructions, abundances of Mediterranean taxa and representation of local/regional pollen signals, this hypothesis may explain the differences in the amplitude of change in vegetation to climate variability observed across the available high-resolution records shown in Figure 7. The changes in forest cover documented in the marine records from ODP976 and U1385, for instance, remain relatively more subdued during both moderate- and high-intensity events compared to Lake Ohrid, where Mediterranean taxa suffer an almost complete disappearance and temperate humid forests undergo much more severe diebacks. At Tenaghi Philippon, high-intensity events seem to impact vegetation at a similar rate to Lake Ohrid, although moderate events do not appear to be as impactful which could be due to the lower altitude of this site (see Tab 1). If the hypothesis that the Balkans were wetter during MIS 11 was correct, this may suggest that vegetation in this region may have reacted more intensely to the impact of cool and especially arid events, while the generally drier conditions in the western Mediterranean and around the Alboran Sea could have benefitted thermophilous vegetation even during harsher climates.

5.4 Implications for hominin populations

Our record from site ODP 976 provides evidence for the strong climatic transition from MIS 12 to MIS 11, which undoubtedly influenced hominin populations across Europe. From around 426 ka BP, after the MIS 12 glaciation, modelled population distributions show demographic expansion across Europe (e.g. Blain *et al.* 2021; Rodríguez *et al.*, 2022). The model by Rodríguez *et al.* (2022), for instance, estimates an increase in total population across Western Europe from a range of ~10,000–90,000 individuals during MIS 12a to ~25,000–

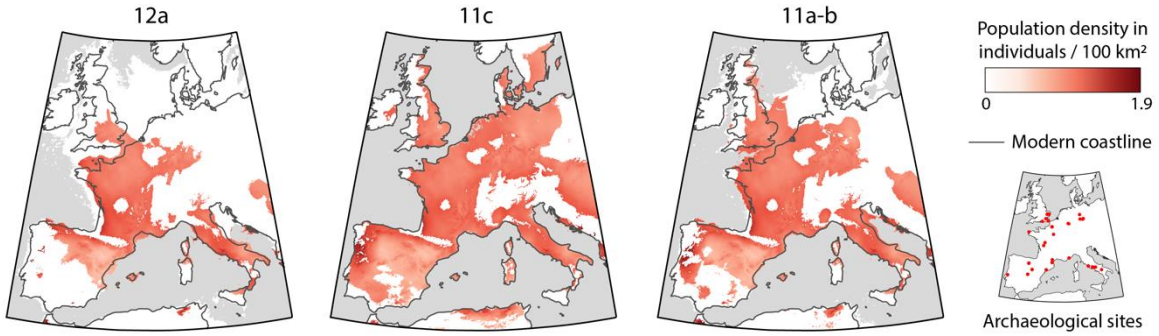

Figure 8 - *Density of hominin populations across Western Europe during substages MIS 12a, MIS 11c and MIS 11a-b (adapted from Rodríguez et al., 2022).*

170,000 individuals during the climatic optimum MIS 11c (Fig. 8). During the transition, archaeological sites show the emergence of new subsistence behaviours and technical innovations (core technologies, increase in light-duty tools), and evidence of an early regionalization of traditions (Moncel *et al.*, 2016, 2020, 2021a,b; García-Medrano *et al.*, 2022a,b). These behavioural changes suggest increased cognition with new skills and social interactions (Moncel *et al.*, 2015; Peretto *et al.*, 2016). The correspondence of such a behavioural threshold with the long and stable climatic amelioration observed during the interglacial MIS 11, especially after the harsh glacial event of MIS 12, leads to the supposition that climatic amelioration may have led to such social and technological innovations. Such a long-lasting interglacial period could have encouraged the expansion of favourable territories for long term occupations of hominins vegetation, fauna and hominin occupation in European temperate and Mediterranean ecosystems (Berger *et al.*, 2003; Raymo and Mitrovica, 2012; Oliveira *et al.*, 2016; Moncel *et al.*, 2018; Blain *et al.*, 2021). In particular, the long and stable climatic optimum of MIS 11c means that hominins would have had a longer time to develop a deeper level of social networks, better understanding of their direct environment and potential uses of raw materials, and possibly the spread of the early use of fire (the burning of fuel in Spain may have only begun after 230 ka BP (Fernández Peris et al. 2012), but there is evidence of charcoal dated to MIS 11 found in fireplaces at Terra Amata in France (Lumley, 2016) and Guado San Nicola in Italy (Lebreton et al., 2019)).

The climatic inferences made on the basis of the arboreal expansion in our pollen data coincide with archaeological finds from Caune de L'Arago in the French Pyrenees, where the faunal spectrum for MIS 11 was characterised by an assemblage indicative of temperate conditions, composed of large herbivorous mammals (reindeer, bison, horse and rhinoceros), carnivores (bears, foxes) and rodents (Barsky *et al.*, 2019). Climatic amelioration during Termination V would have increased the availability of large herbivores and facilitated the demographic expansion and mobility of hominins, favouring the diffusion of behavioural innovations observed during this period.

As Szymanek and Julien (2018) and Blain *et al.* (2021) point out, the most favourable conditions for early hominid settlements comprise a moderately warm and humid climate, usually during the early or late parts of an interglacial but not during the thermal maximum. This might suggest that aridity at higher temperatures could have been a limiting factor for early hominin populations. If, as shown by the comparisons of our pollen data with other records in the region, the southwestern Mediterranean was generally more arid than central and eastern Europe, hominins may have preferred to seek areas with greater moisture availability. This may explain why, in the models by Rodríguez *et al.* (2022) (Fig. 8),

southwestern Iberia is less densely populated than other parts of Europe. However, the authors point out that their model is likely to be influenced by the lack of sites with suitable chronologies in this region, limiting our visualisation of the area actually inhabitable by humans (see Santonja and Pérez-González *et al*., 2010; Yravedra *et al*., 2010; Carrión *et al.,* 2011; Finlayson *et al.,* 2011; Santonja *et al.,* 2014, 2016; Altolaguirre *et al* 2020; Rubio-Jara *et al*., 2016; López-García *et al*., 2021; Moncel *et al.,* 2021a, b*;* García-Medrano *et al*., 2022a; Lockey *et al.,* 2022).

Moncel *et al.* (2018) highlight that the Mediterranean has acted as a refugial area for thermophilous and subtropical taxa throughout the Quaternary. As observed in the ODP976 record, vegetation changes in the southwestern Mediterranean were less intense during periods of millennial-scale climatic variability at the end of the MIS 11c optimum and during MIS 11b and 11a. Therefore, it is possible that the persistence of temperate and Mediterranean vegetation in an 'ecological niche' around the Alboran Sea may have facilitated the cultural and technological transition during MIS 11 by providing a reliable source of subsistence. In contrast, during periods of high climatic variability in NW and Central Europe, hominids would have been affected by the contractions of favourable habitats and thereby limited the spread of technological innovations (Kretzoi and Dobosi 1990; Ashton et al 2011; Ashton and Davis 2021; Rawlinson et al 2022; Hosfield, 2022).

The lack of archaeological sites in this region severely limits our ability to test the validity of this hypothesis, and therefore more work must be undertaken in the southwestern Mediterranean to build a better picture of the spatial distribution of hominins in the southwestern Mediterranean during the MIS 12/11 transition. Improving the coverage of archaeological sites in this region will enable a better understanding of the probability of interactions and interbreeding with other European populations, in turn shedding a light on the role of this region in the development of cultural/technological innovations and the evolution of the Neanderthal lineage.

6. Conclusions

This study presented a new high-temporal resolution palynological record from ODP Site 976 in the Alboran Sea, which encompasses the MIS 12/11 transition and covers the entirety of MIS 11 until the beginning of MIS 10. Our palynological results provide evidence for the strong climatic shift from glacial to interglacial. The transition from *Pinus,* montane and steppic taxa, to an assemblage comprised of forested temperate and Mediterranean taxa, is coeval with major fluctuations in planktonic records (SST and $\delta^{18}O$), a sharp increase in Antarctic CO_2 and CH_4 records. The timing of this shift, observed between 430 and 425 ka BP, was correlated with other pollen and marine proxy records from the Mediterranean and North Atlantic, showing a largely synchronous response across the region to global climatic change.

A climatic optimum for temperate and Mediterranean taxa is documented between 426 and 400 ka BP, which corresponds with the warm substage MIS 11c identified in previous palaeoenvironmental and palaeoclimatic records. The data from ODP976 supports the idea that MIS 11c was an exceptionally prolonged phase, synchronous with maxima in temperature and precipitation, and consistently high greenhouse gas concentrations, likely perpetuated by the unique antiphasing between precession and obliquity that characterised the MIS 11 interglacial.

Following the climatic optimum, a slow cooling trend is marked by millennial-scale climatic variability. These events were recognised as moderate-intensity (no counterpart in marine proxies) and high-intensity (signature in marine and terrestrial records). Of the

moderate climatic oscillations observed in our record, the most notable was linked to the "Older Holstenian Oscillation" during which a minor forest contraction in temperate forests is observed almost ubiquitously around 408 ka BP across European pollen records. Three high-intensity events were identified at ca. 397, 390 and 378 ka BP and were correlated, keeping chronological uncertainties in consideration, with the light-isotopic events (11.24, 11.23 and 11.22) recorded in $\delta^{18}O$ curves from the Mediterranean and North Atlantic, related to changes in the AMOC. Out of these, possibly the strongest contraction occurred during the insolation minimum at the onset of MIS 11b, which corresponds to the light isotopic event 11.24. The amplitude of the vegetation changes observed at ODP976 during the millennial-scale events may be less intense than what has been previously found in the Balkan Peninsula. This may be due to the overall aridity of the western Mediterranean compared to the east, which could have ensured a prolonged resilience of Mediterranean vegetation during colder conditions.

The abrupt shift in vegetation during the MIS12/11 transition and the millennial-scale climatic fluctuations of MIS 11 may be used to infer that hominin populations would have had to adapt to these climatic changes. Climatic amelioration after the harsh glacial of MIS 12 may explain the behavioural threshold observed during the course of the long interglacial MIS 11 and internal variations (MIS 11c *vs*. MIS 11b and 11a). A warmer and wetter climate may have helped the ancestors of the Neanderthal to develop new strategies (subsistence and technological), explaining the population increase and the diffusion of these innovations all over Europe. In the context of the Mediterranean, a generally drier climate during MIS 11 compared to central or eastern Europe could have led to a less variable vegetation cover, thereby providing a more reliable source of sustenance during periods of climatic oscillation and thus further facilitating hominin innovations in this period.

Acknowledgements

We gratefully acknowledge the financial support of the ANR project Neandroots (Agence Nationale de la Recherche, project N° ANR-19-CE27-0011-01), the Muséum national d'Histoire naturelle (MNHN) and Centre National de la Recherche Scientifique (CNRS). Thanks also to the APLF (Association des Palynologues de Langue Française) for granting funds to participate in the 5th MedPalynoS symposium and present the results of this research internationally. Many thanks also to L. Dubost at the UMR 7194 palynology laboratory for the valuable and efficient technical assistance, and Y. Miras for the support and advice provided during this project. Finally, we thank the Ocean Drilling Program for making the samples available for analysis.

References

Alonso, B., Ercilla, G., Martínez-Ruiz, F., Baraza, J., and Galimont, A. (1999). Pliocene-Pleistocene sedimentary facies at Site 976: Depositional history in the northwestern Alboran Sea. *Proceedings of the Ocean Drilling Program: Scientific Results*, 161(1994), 57–68. https://doi.org/10.2973/odp.proc.sr.161.206.1999

Altolaguirre, Y., Bruch, A.A. and Gibert, L. (2020). A long Early Pleistocene pollen record from Baza Basin (SE Spain): Major contributions to the palaeoclimate and palaeovegetation of Southern Europe. *Quaternary Science Reviews* 231, pp.106199.

Ashton, N., & Davis, R. (2021). Cultural mosaics, social structure, and identity: The Acheulean threshold in Europe. *Journal of Human Evolution*, 156, 103011.

Ardenghi, N., Mulch, A., Koutsodendris, A., Pross, J., Kahmen, A., and Niedermeyer, E. M. (2019). Temperature and moisture variability in the eastern Mediterranean region during

758 Marine Isotope Stages 11–10 based on biomarker analysis of the Tenaghi Philippon peat
759 deposit. *Quaternary Science Reviews*, 225.
760 https://doi.org/10.1016/j.quascirev.2019.105977
761 Azibeiro, L. A., Sierro, F. J., Capotondi, L., Lirer, F., Andersen, N., González-Lanchas, A., Alonso-
762 Garcia, M., Flores, J. A., Cortina, A., Grimalt, J. O., Martrat, B. and Cacho, I. (2021).
763 Meltwater flux from northern ice-sheets to the mediterranean during MIS 12. Quaternary
764 Science Reviews, 268. https://doi.org/10.1016/j.quascirev.2021.107108
765 Barber, D.C., Dyke, A., Hillaire-Marcel, C., Jennings, A.E., Andrews, J.T., Kerwin, M.W.,
766 Bilodeau, G., McNeely, R., Southon, J., Morehead, M.D. and Gagnon, J.M. (1999). Forcing
767 of the cold event of 8,200 years ago by catastrophic drainage of Laurentide
768 lakes. *Nature*, 400(6742), pp.344-348.
769 Barbero, M., Quézel, P., Rivas-Martínez, S., 1981. Contribution á l'étude des groupements
770 forestiers et préforestiers du Maroc. *Phytocoenologia* 9, pp.311–412.
771 Barsky, D., Moigne, A. M., and Pois, V. (2019). The shift from typical Western European Late
772 Acheulian to microproduction in unit 'D' of the late Middle Pleistocene deposits of the
773 Caune de l'Arago (Pyrénées-Orientales, France). *Journal of Human Evolution*, 135.
774 https://doi.org/10.1016/j.jhevol.2019.102650
775 Bassinot, F. C., Labeyrie, L. D., Vincent, E., Quidelleur, X., Shackleton, N. J., and Lancelot, Y.
776 (1994). The astronomical theory of climate and the age of the Brunhes-Matuyama mag-
777 netic reversal, *Earth Planet. Sci. Lett*., 126, pp.91–108
778 Benabib, A. (1982). Bref aperçu sur la zonation altitudinale de la végétation climatique du
779 Maroc, *Ecol. Medit*., 8(1–2), pp.301–315.
780 Berger, A. (1978). Long-term variations of daily insolation and Quaternary climatic changes.
781 *Journal of Atmosmospheric Sciences,* 35(12), pp.2362-2367.
782 Berger, A and Loutre, M.F. (1991). Insolation values for the climate of the last 10 million of
783 years. *Quaternary Science Reviews*, 10(4), 297-317.
784 Berger, A. and Loutre M.F. (2003). Climate 400,000 years ago, a key to the future? In: A.W.
785 Droxler, R.Z. *Past Interglacials Working Group of Pages, Interglacials of the last 800,000*
786 *years.* R. of Geop., 54, pp.162-219.
787 Berger, W. H. and Wefer, G. (2003). On the dynamics of the ice ages: Stage-11 paradox, mid-
788 Brunhes climate shift, and 100-ky cycle. *Geophys. Monogr.-Am. Geophys. UNION*, 137,
789 pp.41–60.Blain, H. A., Fagoaga, A., Ruiz-Sánchez, F. J., García-Medrano, P., Ollé, A., and
790 Jiménez-Arenas, J. M. (2021). Coping with arid environments: A critical threshold for
791 human expansion in Europe at the Marine Isotope Stage 12/11 transition? The case of the
792 Iberian Peninsula. *Journal of Human Evolution*, 153.
793 https://doi.org/10.1016/j.jhevol.2021.102950
794 Bout-Roumazeilles, V., Combourieu-Nebout, N., Peyron, O., Cortijo, E., and Masson-Delmotte,
795 V. (2007). Connexion between South Mediterranean climate and North African
796 atmospheric circulation during MIS 3 North Atlantic cold events. *Quaternary Science*
797 *Reviews*, 26, pp.3197–3215.
798 Brandon, M., Landais, A., Duchamp-Alphonse, S., Favre, V., Schmitz, L., Abrial, H., Prié, F.,
799 Extier, T. and Blunier, T. (2020). Exceptionally high biosphere productivity at the beginning
800 of Marine Isotopic Stage 11. *Nature communications*, 11(1), pp.1-10. https://
801 doi.org/10.1038/s41467-020-15739-2.
802 Brice R. (2007) *Variabilité Climatique en Mer d'Alboran au cours de la Teminaison V (MIS*
803 *12/11).* Unpublished thesis, University of Bordeaux.

Bulian, F., Kouwenhoven, T. J., Jiménez-Espejo, F. J., Krijgsman, W., Andersen, N., and Sierro, F. J. (2022). Impact of the Mediterranean-Atlantic connectivity and the late Miocene carbon shift on deep-sea communities in the Western Alboran Basin. *Palaeogeography, Palaeoclimatology, Palaeoecology,* 589. https://doi.org/10.1016/j.palaeo.2022.110841

Candy, I., Schreve, D. C., Sherriff, J., and Tye, G. J. (2014). Marine Isotope Stage 11: Palaeoclimates, palaeoenvironments and its role as an analogue for the current interglacial. *Earth-Science Reviews*, 128, pp.18–51. https://doi.org/10.1016/j.earscirev.2013.09.006

Carrión, José S., James Rose, and Chris Stringer. (2011) Early human evolution in the western Palaearctic: ecological scenarios." *Quaternary Science Reviews*, 30(11-12), pp.1281-1295.

Chaisson, W. P., Poli, M. S., and Thunell, R. C. (2002). Gulf Stream and Western Boundary Undercurrent variations during MIS 10-12 at site 1056, Blake-Bahama Outer Ridge. *Marine Geology*, 189(1–2), pp.79–105. https://doi.org/10.1016/S0025-3227(02)00324-9

Combourieu-Nebout, N., Londeix, L., Baudin, F., Turon, J.-L., von Grafenstein, R., and Zahn, R. (1999). Quaternary marine and continental paleoenvironments in the western Mediterranean (Site 976, Alboran Sea): palynological evidence, in: *Proc. ODP Sci. Results*, 161: College Station, TX (Ocean Drilling Program), edited by: Zahn, R., Comas, M. C., and Klaus, A., pp.457–468.

Combourieu-Nebout, N., Turon, J. L., Zahn, R., Capotondi, L., Londeix, L., and Pahnke, K. (2002). Enhanced aridity and atmospheric high-pressure stability over the western Mediterranean during the North Atlantic cold events of the past 50 k.y. *Geology*, 30(10), pp.863–866. https://doi.org/10.1130/0091-7613(2002)030<0863:EAAAHP>2.0.CO;2

Combourieu-Nebout, N., Peyron, O., Dormoy, I., Desprat, S., Beaudouin, C., Kotthoff, U., and Marret, F. (2009). Rapid climatic variability in the west Mediterranean during the last 25000 years from high resolution pollen data. *Climate of the Past*, 5(3), pp.503–521. https://doi.org/10.5194/cp-5-503-2009

Dahl, E. (1998). *The Phytogeography of Northern Europe (British Isles, Fennoscandia and Adjacent Areas).* Cambridge Univ. Press, UK.

de Kaenel, E., Siesser, W.G., Murat, A. (1999). Pleistocene calcareous nannofossil biostratigraphy and the western Mediterranean sapropels, Sites 974 to 977 and 979. In: Zhan, R., Comas, M.C., Klaus, A. (Eds.), *Proc. ODP Sci*. *Results*., 161. College Station, Texas, pp.15–183

Desprat, S., Sánchez Goñi, M. F., Turon, J. L., McManus, J. F., Loutre, M. F., Duprat, J., Malaizé, B., Peyron, O., and Peypouquet, J. P. (2005). Is vegetation responsible for glacial inception during periods of muted insolation changes? *Quaternary Science Reviews*, 24(12–13), pp.1361–1374. https://doi.org/10.1016/j.quascirev.2005.01.005

Desprat, S., Sánchez Goñi, M. F., Naughton, F., Turon, J. L., Duprat, J., Malaizé, B., Cortijo, E., and Peypouquet, J. P. (2007). Climate variability of the last five isotopic interglacials: Direct land-sea-ice correlation from the multiproxy analysis of North-Western Iberian margin deep-sea cores. *Developments in Quaternary Science*, 7(C), pp.375–386. https://doi.org/10.1016/S1571-0866(07)80050-9

Droxler, A. W., Alley, R. B., Howard, W. R., Poore, R. Z., and Burckle, L. H. (2003). Unique and exceptionally long interglacial marine isotope stage 11: Window into earth warm future climate. *Geophysical Monograph Series*, 137(January 2015), pp.1–14. https://doi.org/10.1029/137GM01

Ellison, C.R.W., Chapman, M.R., Hall, I.R. (2006). Surface and deep ocean interactions during the cold climate event 8200 years ago. *Science* 312, pp.1929–1932.

Faegri, F. and Iversen, J. (1989). *Textbook of Pollen Analysis (4th Edition).* Chichester, UK: John Wiley and Sons.

Fernández Peris, J., Barciela González, V., Blasco, R., Cuartero, F., Fluck, H., Sañudo, P. and Verdasco, C. (2012). The earliest evidence of hearths in Southern Europe: the case of Bolomor Cave (Valencia, Spain). *Quaternary International*, 247, pp.267–277.

Finlayson, C., Carrión, J., Brown, K., Finlayson, G., Sánchez-Marco, A., Fa, D., Rodríguez-Vidal, J., Fernández, S., Fierro, E., Bernal-Gómez, M. and Giles-Pacheco, F. (2011). The Homo habitat niche: using the avian fossil record to depict ecological characteristics of Palaeolithic Eurasian hominins. *Quaternary Science Reviews*, 30(11-12), pp.1525-1532.

Fletcher, W. J. and Sánchez Goñi, M. F. (2008) Orbital- and sub-orbital-scale climate impacts on vegetation of the western Mediterranean basin over the last 48,000 yr. *Quaternary Research,* 70, pp.451–464.

Garcia-Gorriz, E., and Garcia-Sanchez, J. (2007). Prediction of sea surface temperatures in the western Mediterranean Sea by neural networks using satellite observations. *Geophysical research letters*, 34(11).

García-Medrano, P., Despriée, J., Moncel M-H. (2022a). Innovations in Acheulean biface production at la Noira (Centre France): shift or drift between 700 and 450 ka in Western Europe? *Anthropological and Archaeological Sciences*.

García-Medrano, P., Shipton, C., White, M., and Ashton, N. (2022b). Acheulean Diversity in Britain (MIS 15-MIS 11): From the Standardization to the Regionalization of Technology. *Frontiers in Earth Science*, 10, 917207.

Girone, A., Maiorano, P., Marino, M., and Kucera, M. (2013). Calcareous plankton response to orbital and millennial-scale climate changes across the Middle Pleistocene in the western Mediterranean. *Palaeogeography, Palaeoclimatology, Palaeoecology*, 392, pp.105–116. https://doi.org/10.1016/j.palaeo.2013.09.005

González-Donoso, J. M., Serrano, F., and Linares, D. (2000). Sea surface temperature during the Quaternary at ODP Sites 976 and 975 (western Mediterranean). *Palaeogeography, Palaeoclimatology, Palaeoecology*, 162(1–2), pp.17–44. https://doi.org/10.1016/S0031-0182(00)00103-6

Hammer, Ø., Harper, D.A. and Ryan, P.D., 2001. PAST: Paleontological statistics software package for education and data analysis. *Palaeontologia electronica*, 4(1), p.9.

Hes, G., Goñi, M. F. S., and Bouttes, N. (2022). Impact of terrestrial biosphere on the atmospheric CO2concentration across Termination V. *Climate of the Past*, 18(6), pp.1429–1451. https://doi.org/10.5194/cp-18-1429-2022

Hodell, D. A., Channeil, J. E. T., Curtis, J. H., Romero, O. E., and Röhl, U. (2008). Onset of "Hudson Strait" Heinrich events in the eastern North Atlantic at the end of the middle Pleistocene transition (~640 ka)? *Paleoceanography*, 23(4), pp.1–16. https://doi.org/10.1029/2008PA001591

Hosfield, R. (2022). Variations by degrees: Western European paleoenvironmental fluctuations across MIS 13–11. *Journal of Human Evolution*, 169, 103213.

Hrynowiecka, A., Żarski, M., and Drzewicki, W. (2019). The rank of climatic oscillations during MIS 11c (OHO and YHO) and post-interglacial cooling during MIS 11b and MIS 11a in eastern Poland. *Geological Quarterly*, 63(2), pp.375–394. https://doi.org/10.7306/gq.1470

Hublin, J. J. (2009). The origin of Neandertals. *Proceedings of the National Academy of Sciences of the United States of America*, 106(38), pp.16022–16027. https://doi.org/10.1073/pnas.0904119106

Imbrie, J., Hays, J.D., Martinson, D.G., McIntyre, A., Mix, A.C., Morley, J.J., Pisias, N.G., Prell, W.L. and Shackleton, N.J. (1984). The orbital theory of Pleistocene climate: support from a revised chronology of the marine $\delta^{18}O$ record. In: Berger, A.L., Imbrie, J., Hays, J., Kukla, G., Saltzman, B. (Eds.), *Milankovitch and Climate*. D. Reidel, Dordrecht, pp. 269–306.

Jouzel, J., Masson-Delmotte, V., Cattani, O., Dreyfus, G., Falourd, S., Hoffmann, G., Minster, B., Nouet, J., Barnola, J.M., Chappellaz, J., Fischer, H., Gallet, J.C., Johnsen, S., Leuenberger, M., Loulergue, L., Luethi, D., Oerter, H., Parrenin, F., Raisbeck, G., Raynaud, D., Schilt, A., Schwander, J., Selmo, E., Souchez, R., Spahni, R., Stauffer, B., Steffensen, J.P., Stenni, B., Stocker, T.F., Tison, J.L., Werner, M., Wolff, E.W., 2007. Orbital and millennial Antarctic climate variability over the past 800,000 years. Science

Juggins, S. (2020). *Package "rioja" – Analysis of Quaternary Science Data, The Comprehensive R Archive Network.*

Kandiano, E.S., Bauch, H.A., Fahl, K., Helmke, J.P., Röhl, U., Pérez-Folgado, M., Cacho, I. (2012). The meridional temperature gradient in the eastern North Atlantic during MIS 11 and its link to the ocean–atmosphere system. *Palaeogeogr., Palaeoclimatol., Palaeoecol*. 333, pp.24–39.

Kelly, M.R. (1964). The Middle Pleistocene of North Birmingham. *Philos. Trans. R. Soc. Lond.,* B247, pp.533–592.

Kousis, I., Koutsodendris, A., Peyron, O., Leicher, N., Francke, A., Wagner, B., Giaccio, B., Knipping, M., and Pross, J. (2018). Centennial-scale vegetation dynamics and climate variability in SE Europe during Marine Isotope Stage 11 based on a pollen record from Lake Ohrid. *Quaternary Science Reviews*, 190, pp.20–38. https://doi.org/10.1016/j.quascirev.2018.04.014

Koutsodendris, A., Müller, U.C., Pross, J., Brauer, A., Kotthoff, U., Lotter, A.F. (2010). Vegetation dynamics and climate variability during the Holsteinian interglacial based on a pollen record from Dethlingen (northern Germany). *Quaternary Science Reviews* 29, pp.3298–3307

Koutsodendris, A., Brauer, A., Pälike, H., Müller, U.C., Dulski, P., Lotter, A.F., Pross, J. (2011). Sub-decadal to decadal-scale climate cyclicity during the Holsteinian interglacial (MIS 11) evidenced in annually laminated sediments. *Climate of the Past,* 7, pp.987–999.

Koutsodendris, A., Pross, J., Müller, U. C., Brauer, A., Fletcher, W. J., Kühl, N., Kirilova, E., Verhagen, F. T. M., Lücke, A., and Lotter, A. F. (2012). A short-term climate oscillation during the Holsteinian interglacial (MIS 11c): An analogy to the 8.2ka climatic event? *Global and Planetary Change*, 92–93, pp.224–235. https://doi.org/10.1016/j.gloplacha.2012.05.011

Koutsodendris, A., Kousis, I., Peyron, O., Wagner, B., and Pross, J. (2019). The Marine Isotope Stage 12 pollen record from Lake Ohrid (SE Europe): Investigating short-term climate change under extreme glacial conditions. *Quaternary Science Reviews*, 221. https://doi.org/10.1016/j.quascirev.2019.105873

Krtezoi, M. and Dobosi, V.T. (1990). *Vértesszölös Man site and culture*. Akademiai Kiado, Budapest. 554 p.

Kukla, G. (2003). Continental records of MIS 11. *Washington DC American Geophysical Union Geophysical Monograph Series*, 137, pp.207-211.

Laskar, J., Robutel, P., Joutel, F., tineau, M.G., Correia, A.C.M., Levrard, B., Gastineau, M., Correia, A.C.M., Levrard, B. (2004). A long-term numerical solution for the insolation quantities of the earth. *AandA* 428, pp.261-285. https://doi.org/ 10.1051/0004-6361:20041335.

Lebreton, V., Bertini, A., Russo Ermolli, E., Stirparo, C., Orain, R., Vivarelli, M., Combourieu-Nebout, N., Peretto, C. and Arzarello, M. (2019). Tracing fire in early European prehistory: Microcharcoal quantification in geological and archaeological records from Molise (southern Italy). *Journal of Archaeological Method and Theory*, 26, pp.247-275.

Lisiecki, L. E., and Raymo, M. E. (2009). Diachronous benthic $\delta^{18}O$ responses during late Pleistocene terminations. *Paleoceanography*, 24(3).

Lockey, A.L., Rodríguez, L., Martín-Francés, L., Arsuaga, J.L., de Castro, J.M.B, Crété, L., Martinón-Torres, M., Parfitt, S., Pope, M. and Stringer, C. (2022). Comparing the Boxgrove and Atapuerca (Sima de los Huesos) human fossils: Do they represent distinct paleodemes? *Journal of Human Evolution* 172, 103253.

López-García, Juan Manuel, Gloria Cuenca-Bescós, Maria Ángeles Galindo-Pellicena, Elisa Luzi, Claudio Berto, Loïc Lebreton, and Emmanuel Desclaux. "Rodents as indicators of the climatic conditions during the Middle Pleistocene in the southwestern Mediterranean region: implications for the environment in which hominins lived." Journal of Human Evolution 150 (2021): 102911.

Loulergue, L., Schilt, A., Spahni, R., Masson-Delmotte, V., Blunier, T., Lemieux, B., Barnola, J.M., Raynaud, D., Stocker, T.F., Chappellaz, J. (2008). Orbital and millennial-scale features of atmospheric CH_4 over the past 800,000 years. *Nature*, 453, pp.383-386.

Lourens, L.J., 2004. Revised tuning of Ocean Drilling Program Site 964 and KC01B (Mediterranean) and implications for the $\delta^{18}O$, tephra, calcareous nannofossil, and geomagnetic reversal chronologies of the past 1.1 Myr. *Paleoceanography*, 19, pp.1-20. https://doi.org/10.1029/2003PA000997.

Loutre, M.F., Berger, A. (2003). Marine Isotope Stage 11 as an analogue for the present interglacial. *Glob. Planet. Change*, 36, pp.209-217. https://doi.org/10.1016/S0921-8181(02)00186-8

Lumley de H. (2016). *Terra Amata. Nice, Alpes-Maritime, France. Comportement et mode de vie des chasseurs acheuléens de Terra Amata (Tome V).* CNRS Editions.

Magri, D. and Parra, I. (2002). Late Quaternary western Mediterranean pollen records and African winds. *Earth Planet. Sc. Lett.*, 200, 401–408.

Mangili, C., Brauer, A., Plessen, B., Moscariello, A. (2007). Centennial-scale oscillations in oxygen and carbon isotopes of endogenic calcite from a 15,000 varve year record of the Pianico interglacial. *Quat. Sci. Rev.*, 26, pp.1725–1735.

Marino, M., Maiorano, P., Tarantino, F., Voelker, A., Capotondi, L., Girone, A., Lirer, F., Flores, J. A., and Naafs, B. D. A. (2014). Coccolithophores as proxy of seawater changes at orbital-to-millennial scale during middle Pleistocene Marine Isotope Stages 14-9 in North Atlantic core MD01-2446. *Paleoceanography*, 29(6), pp.518–532. https://doi.org/10.1002/2013PA002574

Marino, M., Girone, A., Maiorano, P., Di Renzo, R., Piscitelli, A., and Flores, J. A. (2018). Calcareous plankton and the mid-Brunhes climate variability in the Alboran Sea (ODP Site 977). *Palaeogeography, Palaeoclimatology, Palaeoecology*, 508, pp.91–106. https://doi.org/10.1016/j.palaeo.2018.07.023

Martrat, B., Grimalt, J.O., Shackleton, N.J., de Abreu, L., Hutterli, M.A., Stocker, T.F. (2007). Four climate cycles of recurring deep and surface water destabilizations on the Iberian margin. *Science*., 317(5837), pp.502-507. doi: 10.1126/science.1139994.

McManus, J.F., Oppo, D.W., Cullen, J.L. (1999). A 0.5 million-year record of millennial-scale climate variability in the North Atlantic. *Science* 283, pp.971–975.

McManus, J.F., Oppo, D.W., Cullen, J.L. and Healey, S. (2003). Marine isotope stage 11 (MIS 11): analog for Holocene and future Climate? *Washington DC American Geophysical Union Geophysical Monograph Series*, 137, pp.69-85.

Moncel, M.H., Ashton, N., Lamotte, A., Tuffreau, A., Cliquet, D. and Despriée, J. (2015). The early Acheulian of north-western Europe. *Journal of Anthropological Archaeology*, 40, pp.302-331.

Moncel, M. H., Arzarello, M., and Peretto, C. (2016). The Hoslteinian period in Europe (MIS 11-9). *Quaternary International*, 409, pp.1–8. https://doi.org/10.1016/j.quaint.2016.06.006

Moncel, M. H., Landais, A., Lebreton, V., Combourieu-Nebout, N., Nomade, S., and Bazin, L. (2018). Linking environmental changes with human occupations between 900 and 400 ka in Western Europe. *Quaternary International*, 480, pp.78–94. https://doi.org/10.1016/j.quaint.2016.09.065

Moncel M-H., Biddittu I., Manzi G., Saracino B., Pereira A., Nomade S., Hertler C., Voinchet P., Bahain J-J. (2020) Emergence of regional cultural traditions during the Lower Paleolithic: evidence of a network of sites at the MIS 11-10 transition in Central Italy (Frosinone-Ceprano basin). *Anthropological and archaeological sciences,* 12(8), pp.1-32.

Moncel M-H., García-Medrano, P., Despriée, J., Arnaud, J., Voinchet, P., Bahain J-J. (2021a). Tracking behavioral persistence and innovations during the Middle Pleistocene in Western Europe. Shift in occupations between 700 ka and 450 ka at la Noira site (Centre, France). *Journal of Human Evolution.* Humans in transition special issue 156, 103009. https://doi.org/10.1016/j.jhevol.2021.103009

Moncel M-H., Ashton N., Arzarello M., Fontana F., Lamotte A., Scott B., Muttillo B., Berruti B., Nenzioni G., Tuffreau A., Peretto C. (2021b). An Early Levallois core technology between MIS 12 and 9 in Western Europe? *Journal of Human Evolution,* 139, 102735.

Nehrbass-Ahles, C., Shin, J., Schmitt, J., Bereiter, B., Joos, F., Schilt, A., Schmidely, L., Silva, L., Teste, G., Grilli, R. and Chappellaz, J., (2020). Abrupt CO_2 release to the atmosphere under glacial and early interglacial climate conditions. *Science*, 369(6506), pp.1000-1005.

Okuda, M., Yasuda, Y., Setoguchi, T. (2001). Middle to late Pleistocene vegetation history and climatic changes at Lake Kopais, southeast Greece. *Boreas,* 30, 73-82.

Oliveira, D., Desprat, S., Rodrigues, T., Naughton, F., Hodell, D., Trigo, R., Rufino, M., Lopes, C., Abrantes, F., and Sánchez Goñi, M. F. (2016). The complexity of millennial-scale variability in southwestern Europe during MIS 11. *Quaternary Research* (United States), 86(3), pp.373–387. https://doi.org/10.1016/j.yqres.2016.09.002

Olson, S.L., Hearty, P.J.A. (2009). A sustained 121m sea level highstand during MIS 11 (400 ka): direct fossil and sedimentary evidence from Bermuda. *Quat. Sci. Rev.* 28, pp.271–285.

Oppo, D.W., McManus, J., Cullen, J.C. (1998). Abrupt climate change events 500,000 to 340,000 years ago: evidence from subpolar North Atlantic sediments. *Science*, 279, 1335–1338.

Ozenda, P. (1975). Sur les étages de végétation dans les montagnes du bassin méditerranéen. *Documents de Cartographie Ecologique*, 16, pp.1–32.

Parada, M. and Canton, M. (1998). Sea surface temperature variability in Alboran Sea from satellite data. *International Journal of Remote Sensing*, 19(13), pp.2439-2450.

Peretto, C., Arzarello, M., Bahain, J.J., Boulbes, N., Dolo, J.M., Douville, E., Falguéres, C., Frank, N., García, T., Lembo, G., Moigne, A.M., Muttillo, B., Nomade, S., Pereira, A., Rufo, M.A., Sala, B., Shao, Q., Thun Hohenstein, U., Tessari, U., Chiara Turrini, M., Vaccaro, C. (2016).

The Middle Pleistocene site of Guado San Nicola (Monteroduni, Central Italy) on the Lower/Middle Palaeolithic transition. *Quaternary International,* 411, pp.301-315.

Pierre, C., Belanger, P., Saliege, J.F., Urrutiaguer, M.J., Murat, A. (1999). Paleoceanography of the western Mediterranean during the Pleistocene: oxygen and carbon isotope records at site 975. In: Zahn, R., Comas, M.C., Klaus, A. (Eds.). *Proceedings of the Ocean Drilling Program, Scientific Results, 161*. ODP, College Station, Texas, pp.481–488.

Pross, J., Koutsodendris, A., Christanis, K., Fischer, T., Fletcher, W.J., Hardiman, M., Kalaitzidis, S., Knipping, M., Kotthoff, U., Milner, A.M. (2015). The 1.35-Ma-long terrestrial climate archive of Tenaghi Philippon, northeastern Greece: evolution, exploration, and perspectives for future research. *Newsletters Stratigr*. 48, pp.253-276.

Punt, W., and Blackmore, S. (1991). Oleaceae. *Review of Palaeobotany and Palynology*, 69(1–3), pp.23–47. https://doi.org/10.2307/4113622

Quézel, P. and Médail, F., (2003). *Ecologie et biogéographie des forêts du basin méditerranéen*, Elsevier-Lavoisier eds, Paris, France, 571 pp.

Railsback, L.B., Gibbard, P.L., Head, M.J., Voarintsoa, N.R.G., Toucanne, S. (2015). An optimized scheme of lettered marine isotope substages for the last 1.0 million years, and the climatostratigraphic nature of isotope stages and substages. *Quat. Sci. Rev*. 111, pp.94-106. https://doi.org/10.1016/j.quascirev.2015.01.012.

Rawlinson, A., Dale, L., Ashton, N., Bridgland, D. and White, M. (2022): Flake tools in the European Lower Paleolithic: A case study from MIS 9 Britain. Journal of Human Evolution 165, 103153.

Raymo, M.E. and Mitrovica, J.X. (2012). Collapse of polar ice sheets during the stage 11 interglacial. *Nature*, 483(7390), pp.453-456.

Regattieri, E., Giaccio, B., Galli, P., Nomade, S., Peronace, E., Messina, P., Sposato, A., Boschi, C., and Gemelli, M. (2016). A multi-proxy record of MIS 11-12 deglaciation and glacial MIS 12 instability from the Sulmona basin (central Italy). *Quaternary Science Reviews*, 132, pp.129–145. https://doi.org/10.1016/j.quascirev.2015.11.015

Reille, M., de Beaulieu, J-L. (1990). Pollen analysis of a long Upper Pleistocene continental sequence in a Velay maar (Massif Central, France). *Palaeogeography Palaeoclimatology Palaeoecology*, 80, pp.35–48.

Reille, M., and de Beaulieu, J. L. (1995). Long Pleistocene pollen records from the Praclaux crater, south-central France. *Quaternary Research*, 44(2), pp. 205–215. https://doi.org/10.1006/qres.1995.1065

Reille, M., Andrieu, V., de Beaulieu, J.-L., Guenet, P., Goeury, C. (1998). A long pollen record from Lac du Bouchet, Massif Central, France for the period 325 to 100 ka (OIS 9c to OIS 5e). *Quaternary Science Reviews*, 17, pp,1107–1123.

Rivas-Martínez, S. (1982). Bioclimatic stages, chorological sectors and series of vegetation in Mediterranean Spain. *Ecologia mediterranea* , 8(1), pp.275-288.

Rodrigues, T., Voelker, A. H. L., Grimalt, J. O., Abrantes, F., and Naughton, F. (2011). Iberian Margin sea surface temperature during MIS 15 to 9 (580-300 ka): Glacial suborbital variability versus interglacial stability. *Paleoceanography*, 26(1), pp.1–16. https://doi.org/10.1029/2010PA001927

Rodríguez, J., Burjachs, F., Cuenca-Bescós, G., García, N., Van der Made, J., González, A.P., Blain, H.A., Expósito, I., López-García, J.M., Antón, M.G. and Allué, E. (2011). One million years of cultural evolution in a stable environment at Atapuerca (Burgos, Spain). *Quaternary Science Reviews*, 30(11-12), pp.1396-1412.

Rodríguez, J., Willmes, C., Sommer, C., & Mateos, A. (2022). Sustainable human population density in Western Europe between 560.000 and 360.000 years ago. *Scientific Reports*, 12(1), pp.6907.

Rubio-Jara, S., Panera, J., Rodríguez-de-Tembleque, J., Santonja, M. and Pérez-González, A. (2016.) Large flake Acheulean in the middle of Tagus basin (Spain): Middle stretch of the river Tagus valley and lower stretches of the rivers Jarama and Manzanares valleys. *Quaternary international*, 411, pp.349-366.

Sadori, L., Koutsodendris, A., Panagiotopoulos, K., Masi, A., Bertini, A., Combourieu-Nebout, N., Francke, A., Kouli, K., Joannin, S., Mercuri, A.M. and Peyron, O. (2016). Pollen-based paleoenvironmental and paleoclimatic change at Lake Ohrid (south-eastern Europe) during the past 500 ka. *Biogeosciences*, 13(5), pp.1423-1437.

San-Miguel-Ayanz, J., de Rigo, D., Caudullo, G., Houston Durrant, T., Mauri, A. (2016). *European Atlas of Forest Tree Species.* Publication Office of the European Union, Luxembourg.

Sánchez Goñi, M.F. (2022). *The climatic and environmental context of the Late Pleistocene. In Updating Neanderthals*. Academic Press, pp. 17-38.

Sánchez Goñi, M., Eynaud, F., Turon, J. L., and Shackleton, N. J. (1999). High resolution palynological record off the Iberian margin: direct land-sea correlation for the Last Interglacial complex. *Earth and Planetary Science Letters*, 171(1), pp.123-137.

Sánchez Goñi, M.F., Landais, A., Cacho, I., Duprat, J., Rossignol, L. (2009). Contrasting intrainterstadial climatic evolution between high and middle North Atlantic latitudes: a close-up of Greenland interstadials 8 and 12. *Geochemistry, Geophysics, Geosystems*, 10. http://dx.doi.org/10.1029/2008GC002369

Sánchez Goñi, M. F., Llave, E., Oliveira, D., Naughton, F., Desprat, S., Ducassou, E., Hodell, D. A., and Hernández-Molina, F. J. (2016). Climate changes in southwestern Iberia and Mediterranean Outflow variations during two contrasting cycles of the last 1 Myrs: MIS 31-MIS 30 and MIS 12-MIS 11. *Global and Planetary Change*, 136, pp.18–29. https://doi.org/10.1016/j.gloplacha.2015.11.006

Santonja, M. and Pérez-González, A. (2010). Mid-pleistocene acheulean industrial complex in the Iberian Peninsula." *Quaternary International* 223, pp.154-161.

Santonja, M., Pérez-González, A., Domínguez-Rodrigo, M., Panera, J., Rubio-Jara, S., Sesé, C., Soto, E., Arnold, L.J., Duval, M., Demuro, M. and Ortiz, J.E. (2014). The Middle Paleolithic site of Cuesta de la Bajada (Teruel, Spain): a perspective on the Acheulean and Middle Paleolithic technocomplexes in Europe. *Journal of Archaeological Science*, 49, pp.556-571.

Santonja, M., Pérez-González, A., Panera, J., Rubio-Jara, S., and Méndez-Quintas, E. (2016). The coexistence of Acheulean and Ancient Middle Palaeolithic techno-complexes in the Middle Pleistocene of the Iberian Peninsula. *Quaternary International*, 411, pp.367-377.

Shipboard Scientific Party, (1996). Site 976. In: Comas, M.C., Zahn, R., Klaus, A., *et al.*, *Proc. ODP, Init. Repts.*, *161*: College Station, TX (Ocean Drilling Program), pp.179−297.

Suc, J. P. (1984). Origin and evolution of the Mediterranean vegetation and climate in Europe. *Nature*, *307*(5950), pp.429-432.

Szymanek, M. and Julien, M.A. (2018). Early and Middle Pleistocene climate-environment conditions in Central Europe and the hominin settlement record. *Quaternary Science Reviews*, 198, pp.56-75.

Toucanne, S., Zaragosi, S., Bourillet, J.F., Gibbard, P.L., Eynaud, F., Giraudeau, J., Turon, J.-L., Cremer, M., Cortijo, E., Martínez, P., Rossignol, L. (2009). A 1.2 Ma record of glaciation and fluvial discharge from the West European Atlantic margin. *Q. Sci. Rev.* 28, pp.2974–2981

Turner, C. (1970). The middle Pleistocene deposits at marks Tey, Essex. *Phil. Trans. R. Soc. B.,* 257, pp.373-437.

Tye, J., Sherriff, J., Candy, I., Coxon, P., Palmer, A., McClymont, E.L. and Schreve, D.C. (2016). The δ18O stratigraphy of the Hoxnian lacustrine sequence at Marks Tey, Essex, UK: implications for the climatic structure of MIS 11 in Britain. *Journal of Quaternary Science,* 31(2), pp.75-92.

Tzedakis, P.C. (1993). Long-term tree populations in northwest Greece through multiple Quaternary climatic cycles. *Nature,* 364, pp.437–440.

Tzedakis, P.C. (1994). Vegetation change through glacial-interglacial cycles: a long pollen sequence perspective. *Philosophical Transactions Royal Society London*, B 345, pp.403–432

Tzedakis, P. C., Andrieu, V., de Beaulieu, J. L., Crowhurst, S., Follieri, M., Hooghiemstra, H., Magri, D., Reille, M., Sadori, L., Shackleton, N. J., and Wijmstra, T. A. (1997). Comparison of terrestrial and marine records of changing climate of the last 500,000 years. *Earth Planet. Sci. Lett*., 150, pp.171–176.

Tzedakis, P. C., Andrieu, V., de Beaulieu, J. L., Birks, H. J. B., Crowhurst, S., Follieri, M., Hooghiemstra, H., Magri, D., Reille, M., Sadori, L., Shackleton, N. J., and Wijmstra, T. A. (2001). Establishing a terrestrial chronological framework as a basis for biostratigraphical comparisons. *Quaternary Science Reviews*, 20(16–17), pp.1583–1592. https://doi.org/10.1016/S0277-3791(01)00025-7.

Tzedakis, P. C., Hooghiemstra, H., and Pälike, H. (2006). The last 1.35 million years at Tenaghi Philippon: revised chronostratigraphy and long-term vegetation trends. *Quaternary Science Reviews*, 25(23–24), pp.3416–3430. https://doi.org/10.1016/j.quascirev.2006.09.002

Tzedakis, P. C., Pälike, H., Roucoux, K. H., and de Abreu, L. (2009). Atmospheric methane, southern European vegetation and low-mid latitude links on orbital and millennial timescales. *Earth Planet. Sci. Lett*., 277, pp.307–317

Tzedakis, P. C., Hodell, D. A., Nehrbass-Ahles, C., Mitsui, T., and Wolff, E. W. (2022). Marine Isotope Stage 11c: An unusual interglacial. *Quaternary Science Reviews*, 284, 107493. https://doi.org/10.1016/j.quascirev.2022.107493

Vakhrameeva, P., Koutsodendris, A., Wulf, S., Fletcher, W. J., Appelt, O., Knipping, M., Gertisser, R., Trieloff, M., and Pross, J. (2018). The cryptotephra record of the Marine Isotope Stage 12 to 10 interval (460–335 ka) at Tenaghi Philippon, Greece: Exploring chronological markers for the Middle Pleistocene of the Mediterranean region. *Quaternary Science Reviews*, 200, pp.313–333. https://doi.org/10.1016/j.quascirev.2018.09.019

Vázquez Riveiros, N., Waelbroeck, C., Skinner, L., Duplessy, J. C., McManus, J. F., Kandiano, E. S., and Bauch, H. A. (2013). The "MIS 11 paradox" and ocean circulation: Role of millennial scale events. *Earth and Planetary Science Letters*, 371–372, pp.258–268. https://doi.org/10.1016/j.epsl.2013.03.036

Voelker, A. H. L., Rodrigues, T., Billups, K., Oppo, D., McManus, J., Stein, R., Hefter, J., and Grimalt, J. O. (2010). Variations in mid-latitude North Atlantic surface water properties during the mid-Brunhes (MIS 9-14) and their implications for the thermohaline circulation. *Climate of the Past*, 6(4), pp.531–552. https://doi.org/10.5194/cp-6-531-2010

1172 von Grafenstein, U, Erlenkeuser, H., Brauer, A., Jouzel, J. and Johnsen, S.J. (1999). A mid-
1173 European decadal isotope-climate record from 15,500 to 5000 years
1174 BP. *Science*, 284(5420), pp.1654-1657.
1175 Wagner, B., Vogel, H., Francke, A., Friedrich, T., Donders, T., Lacey, J.H., Leng, M.J., Regattieri,
1176 E., Sadori, L., Wilke, T. and Zanchetta, G. (2019). Mediterranean winter rainfall in phase
1177 with African monsoons during the past 1.36 million years. *Nature*, 573(7773), pp.256-260.
1178 West, R.G. (1956). The Quaternary deposits of Hoxne, Suffolk. *Philosophical Transactions of*
1179 *the Royal Society of London, Series*, B 239, pp.265–356.
1180 Wijmstra, T.A., Smit, A. (1976). Palynology of the middle part (30 to 78m) of the 120m deep
1181 section in Northern Greece (Macedonia). *Acta Botanica Neerlandica* 25, pp.297–312.
1182 Yravedra, J., Domínguez-Rodrigo, M., Santonja, M., Pérez-González, A., Panera, J., Rubio-Jara,
1183 S. and Baquedano E. (2010). Cut marks on the Middle Pleistocene elephant carcass of
1184 Áridos 2 (Madrid, Spain). *Journal of Archaeological Science,* 37(10), pp.2469-2476.
1185
1186